THE UNIVERSITY OF RHODE ISLAND

University of Rhode Island
DigitalCommons@URI

Graduate School of Oceanography Faculty Publications

Graduate School of Oceanography

2003

Springtime photochemistry at northern mid and high latitudes

Yuhang Wang

Brian Ridley

See next page for additional authors

Follow this and additional works at: https://digitalcommons.uri.edu/gsofacpubs

Authors

Yuhang Wang, Brian Ridley, Alan Fried, Christopher Cantrell, Douglas Davis, Gao Chen, Julie Snow, Brian G. Heikes, Robert Talbot, Jack Dibb, Frank Flocke, Andrew Weinheimer, Nicola Blake, Donald Blake, Richard Shetter, Barry Lefer, Elliot Atlas, Michael Coffey, Jim Walega, and Brian Wert

Springtime photochemistry at northern mid and high latitudes

Yuhang Wang,[1] Brian Ridley,[2] Alan Fried,[2] Christopher Cantrell,[2] Douglas Davis,[1] Gao Chen,[1] Julie Snow,[3] Brian Heikes,[3] Robert Talbot,[4] Jack Dibb,[4] Frank Flocke,[2] Andrew Weinheimer,[2] Nicola Blake,[5] Donald Blake,[5] Richard Shetter,[2] Barry Lefer,[2] Elliot Atlas,[2] Michael Coffey,[2] Jim Walega,[2] and Brian Wert[2]

[1] Physical and chemical properties of the atmosphere at 0–8 km were measured during the Tropospheric Ozone Production about the Spring Equinox (TOPSE) experiments from February to May 2000 at mid (40°–60°N) and high latitudes (60°–80°N). The observations were analyzed using a diel steady state box model to examine HO_x and O_3 photochemistry during the spring transition period. The radical chemistry is driven primarily by photolysis of O_3 and the subsequent reaction of $O(^1D)$ and H_2O, the rate of which increases rapidly during spring. Unlike in other tropospheric experiments, observed H_2O_2 concentrations are a factor of 2–10 lower than those simulated by the model. The required scavenging timescale to reconcile the model overestimates shows a rapid seasonal decrease down to 0.5–1 day in May, which cannot be explained by known mechanisms. This loss of H_2O_2 implies a large loss of HO_x resulting in decreases in O_3 production (10–20%) and OH concentrations (20–30%). Photolysis of CH_2O, either transported into the region or produced by unknown chemical pathways, appears to provide a significant HO_x source at 6–8 km at high latitudes. The rapid increase of in situ O_3 production in spring is fueled by concurrent increases of the primary HO_x production and NO concentrations. Long-lived reactive nitrogen species continue to accumulate at mid and high latitudes in spring. There is a net loss of NO_x to HNO_3 and PAN throughout the spring, suggesting that these long-term NO_x reservoirs do not provide a net source for NO_x in the region. In situ O_3 chemical loss is dominated by the reaction of O_3 and HO_2, and not that of $O(^1D)$ and H_2O. At midlatitudes, there is net in situ chemical production of O_3 from February to May. The lower free troposphere (1–4 km) is a region of significant net O_3 production. The net production peaks in April coinciding with the observed peak of column O_3 (0–8 km). The net in situ O_3 production at midlatitudes can explain much of the observed column O_3 increase, although it alone cannot explain the observed April maximum. In contrast, there is a net in situ O_3 loss from February to April at high latitudes. Only in May is the in situ O_3 production larger than loss. The observed continuous increase of column O_3 at high latitudes throughout the spring is due to transport from other tropospheric regions or the stratosphere not in situ photochemistry. *INDEX TERMS:* 0317 Atmospheric Composition and Structure: Chemical kinetic and photochemical properties; 0322 Atmospheric Composition and Structure: Constituent sources and sinks; 0365 Atmospheric Composition and Structure: Troposphere—composition and chemistry; 0368 Atmospheric Composition and Structure: Troposphere—constituent transport and chemistry; *KEYWORDS:* springtime, ozone, HO_x, oxidation, reactive nitrogen

[1]School of Earth and Atmospheric Sciences, Georgia Institute of Technology, Atlanta, Georgia, USA.
[2]National Center for Atmospheric Research, Boulder, Colorado, USA.
[3]Graduate School of Oceanography, University of Rhode Island, Narragansett, Rhode Island, USA.
[4]Institute for the Study of Earth, Oceans, and Space, University of New Hampshire, Durham, New Hampshire, USA.
[5]Department of Chemistry, University of California at Irvine, Irvine, California, USA.

1. Introduction

[2] Oxidation processes in the troposphere are important pathways that mitigate the effects of human activities on the environment. These processes are intertwined in a tightly coupled photochemical system that involves among others HO_x (OH + HO_2), O_3, NO_x (NO + NO_2), CO, and hydrocarbons. Spring at northern mid and high latitudes is a particularly interesting and challenging time to study the system because of the rapidly changing photochemical environment driven in part by increasing solar insolation.

[3] Previous understanding for the spring period is largely based on surface measurements and ozonesondes. *Logan* [1985] showed on the basis of ozonesonde measurements a ubiquitous springtime O_3 maximum in the lower troposphere at remote northern mid and high latitude sites. The springtime O_3 maximum at rural sites is in contrast to the summertime O_3 maximum at polluted sites. Two factors have been attributed to the observed springtime ozone maximum, O_3 transport from the stratosphere [*Logan*, 1985; *Levy et al.*, 1985] and O_3 production within the troposphere [*Penkett and Brice*, 1986; *Liu et al.*, 1987]. Measurements in the Swiss Alps (at an altitude of 3.6 km) from the Free Tropospheric Experiment (FREETEX'96 and 98) suggested that the net in situ chemical production of O_3 contributes significantly to the observed spring-summer maximum in the region [*Carpenter et al.*, 2000; *Zanis et al.*, 2000]. Among global 3-D modeling studies of tropospheric O_3, *Wang et al.* [1998] and *Yienger et al.* [1999] investigated in detail the sources of the observed springtime O_3 maximum. While the former study showed that both factors contributed to the simulated springtime O_3 maximum with one peaking in early spring and the other peaking in early summer, the latter study emphasized the effect of net O_3 chemical production at midlatitudes. Possible accumulation of pollutants at high latitudes in winter [*Honrath and Jaffe*, 1992; *Jobson et al.*, 1994; *Novelli et al.*, 1994; *Bottenheim and Shepherd*, 1995; *Honrath et al.*, 1996] may also enhance photochemistry in spring at mid and high latitudes.

[4] The Tropospheric Ozone Production about the Spring Equinox (TOPSE) experiment took place in February–May 2000 (E. Atlas et al., The TOPSE experiment: Introduction, submitted to *Journal of Geophysical Research*, 2002, hereinafter referred to as Atlas et al., submitted manuscript, 2002). Forty two C-130 flights (including 4 test flights) in between Jeffco, Winnipeg, Churchill, and Thule were conducted in 7 deployments, 1–2 weeks apart. A broad suite of in situ measurements of meteorological parameters, trace gases, and aerosols were made from near the surface up to 8 km. The seasonal span of the experiment allows for analyzing the springtime evolution of photochemistry at northern mid and high latitudes.

[5] We describe in section 2 the model and data processing procedures used in this work. In section 3 we examine various aspects of HO_x chemistry. Contributions of primary HO_x production and NO_x concentrations to in situ O_3 production are investigated in section 4. Budgets of reactive nitrogen and O_3 are studied in section 5 to explore the sources of observed O_3 and NO_x. We summarize our findings in section 6.

2. Model Description and Data Processing

[6] A box model is applied in the analysis of in situ photochemistry. The model has been used previously in analyzing observations from other aircraft missions [*Davis et al.*, 1996, 2001; *Crawford et al.*, 1997, 1999; *Chen et al.*, 2001]. The kinetics data for O_3-NO_x-CO-hydrocarbon reactions are taken from *DeMore et al.* [1997] and *Atkinson et al.* [1997]. *Crawford et al.* [1999] listed the reaction rate constants used in the model. Photolysis rate coefficients are first computed using the DISORT 4-stream NCAR Tropospheric

Ultraviolet-Visible (TUV) radiative transfer code (by S. Madronich). The quantum yield and absorption cross-section data are those reported by *DeMore et al.* [1997]; the quantum yield of $O(^1D)$ is from *Talukdar et al.* [1998]. The photolysis rates are then constrained by the observed J values [*Shetter et al.*, 2002] to account for cloud and surface reflectivity.

[7] The model is constrained by the observations of O_3, NO, CO, nonmethane hydrocarbons (NMHCs), temperature, and water vapor. Concentrations of H_2O_2, CH_3OOH, and CH_2O are constrained in some simulations (see figure captions for details). All model parameters except NO and photolysis rates are held constant in multiple-day runs. The concentrations of NO_x (NO + NO_2) are held at constant values that give the observed NO concentrations at the time of the observation. The model converges and results are reported when the diurnal cycles of calculated concentrations do not vary from day to day.

[8] Measurement techniques and related data issues are discussed in the companioning papers in the special issue (see Atlas et al. (submitted manuscript, 2002) for a guide). The 1-min merged data file (courtesy of L. Emmons) is used except the data for CH_2O. The updated data [*Fried et al.*, 2002], where the interference from CH_3OH was removed, are used. Observations that show the imprints of Br and Cl chemistry are removed by eliminating data points with O_3 concentrations <20 ppbv or depleted C_2H_2 relative to benzene [*Jobson et al.*, 1994]; these data were found at altitudes of <1 km above the surface. Data points with O_3 concentrations > 100 ppbv are also eliminated to remove the influence of stratospheric air masses.

[9] Concentrations of CO were measured with two different instruments. The whole air samples were collected and analyzed later using gas chromatographic apparatus [*Blake et al.*, 2002] (hereafter UCI CO). The sampling frequency is 1–5 min. A fast-response 1 Hz tunable diode laser system from NCAR (hereafter NCAR CO) was also employed. The sensitivity of the instrument is about 1 ppbv for the 30-sec averages reported. Measurements of this instrument are in good agreement with limited whole air canister samples analyzed by gas chromatography at NCAR (M. T. Coffey, personal communication, 2001). However, the UCI CO data are on average 8 ppbv lower than NCAR CO measurements. The root mean square of the difference is 14 ppbv. The reasons for the discrepancies between the two measurements are unclear. In our analysis, we use both measurements to increase the available pool of measured data. When both measurements are available, averages are used.

[10] Acetone was not measured during TOPSE. We applied the observed acetone-CO correlations during the SONEX experiment [*Singh et al.*, 2000]. A least squares fit of SONEX observations at 2–7 km gives [acetone] = 8 + 6.8 ([CO] − 10), where acetone is in pptv and CO is in ppbv. NMHCs and CO were measured using the whole air samples [*Blake et al.*, 2002]. The relatively low sampling frequency of NMHCs reduced the available data points by half in the photochemical analysis. We made use of the faster-response NCAR CO measurements to estimate NMHC concentrations in a similar manner as in estimating acetone concentrations. We first find the least squares fits of NMHCs to NCAR CO and then interpolate NMHC con-

centrations for the NCAR CO data that do not overlap with the NMHC measurements. The fitting and interpolation are conducted for each month in two regions ($40°–60°N$ and $60°–80°N$) for each 2-km altitude bin from 0 to 8 km since much of our analysis in the following sections focuses on the monthly and regional characteristics. The procedure doubles the availability of measurement points, providing better statistical significance of the median values of key variables discussed in the following sections. The uncertainties introduced in these procedures will be taken into account in the analysis.

3. Odd Hydrogen

[11] Hydroxyl radicals are central to oxidation chemistry in the troposphere. Their chemical cycles are intrinsically connected to those of O_3. Carbon monoxide, CH_4, and NMHCs are oxidized by OH and peroxy radicals are produced. Peroxy radicals are recycled back to OH by NO, which is oxidized to NO_2. The oxidation cycle leads to O_3 production by NO_2 photolysis. Generally speaking, higher concentrations of O_3 and NO tend to increase OH concentrations and higher concentrations of CO and hydrocarbons tend to decrease OH concentrations. Figure 1 shows the observed monthly median profiles of O_3, NO, C_2H_2, and CO for mid ($40°–60°N$) and high latitudes ($60°–80°N$). Median concentrations of O_3 are comparable between mid and high latitudes. The increase of $10–30$ ppbv O_3 from February to May is more pronounced at high latitudes. Concentrations of NO are much higher at midlatitudes, where the seasonal increase is about a factor of 2 ($10–30$ pptv); the seasonal increase of NO at high latitudes is a factor of $3–5$ (about 10 pptv). In comparison, concentrations of C_2H_2 show a large seasonal decrease by a factor of $2–3$ from February to May. This decrease was also observed for the concentrations of other NMHCs. There is a general decreasing trend for CO; however the trend is much smaller than that of C_2H_2, reflecting in part that photochemistry is both a source and sink for CO but only a sink for NMHCs. The dichotomy in the seasonal trends of O_3 and NO as compared to those of NMHCs and CO signifies the rapid increase of photochemical activity in springtime.

[12] Figure 2 shows simulated monthly median profiles of 24-hour average OH at mid and high latitudes. The model is constrained by observed peroxide concentrations. Only model results are shown because available OH measurements are limited to altitudes below 3 km and the overlapping measurement and simulation data points are few. The concentrations of OH increase significantly through the spring. Their values at high latitudes are significantly less than at midlatitudes reflecting in part the regional difference in solar irradiance and NO concentrations.

[13] Observed and simulated concentrations of total peroxy radicals ($RO_2 = HO_2 +$ organic peroxy radicals) show a similar seasonal trend as OH (Figure 3). Simulated RO_2 concentrations are generally in good agreement with the observations although the model results are too high at midlatitudes in March. Among peroxy radicals, HO_2 and CH_3O_2 are the major components. Detailed analysis of peroxy radical chemistry is carried out by *Cantrell et al.* [2002]. Comparison between simulated and observed HO_2

concentrations is not made since <20 observational data points are available.

3.1. Slowdown of HO$_x$ Cycles: Heterogeneous Loss of H$_2$O$_2$

[14] We use the model to examine the cycling of odd hydrogen. The largest primary source of HO_x in the troposphere is by photolysis of O_3 and the subsequent reaction of $O(^1D)$ and H_2O [*Logan et al.*, 1981]. This source is considered a primary source because its magnitude is largely independent of the HO_x cycling. In comparison, H_2O_2, CH_3OOH, and other peroxides are produced chemically from the reaction of HO_2 and another peroxy radical, both of which are produced during OH oxidation of CO and hydrocarbons. Their photolysis cycles peroxides back to HO_x and provides large HO_x sources. They are generally considered secondary HO_x sources because of their large dependence on OH oxidation. Photolysis of CH_2O is generally considered a secondary source because CH_2O is largely produced from hydrocarbon oxidation, whereas photolysis of acetone is generally a primary source [*McKeen et al.*, 1997].

[15] Figure 4 shows the seasonal profiles of main HO_x sources (24-hour averages) at mid and high latitudes. The three dominant HO_x sources are $O(^1D) + H_2O$ and photolysis of CH_2O and CH_3OOH. The latter two sources are particularly important at high altitudes. The large seasonal increase in the rate of $O(^1D) + H_2O$ is due the increase of solar insolation, O_3 concentrations (Figure 1), and H_2O content of the atmosphere (not shown). The last factor is associated with the seasonal warming of the atmosphere, which increases the saturation vapor pressure. We will show that most of CH_2O and CH_3OOH concentrations are produced by in situ photochemistry. Therefore these two photolysis sources are largely secondary. As a result, the activation of photochemistry in early spring at midlatitudes and in late spring at high latitudes, as evidenced in the seasonal increase of OH and RO_2 concentrations (Figures 2 and 3), is largely driven by the radical source of O_3 photolysis followed by the reaction of $O(^1D)$ and H_2O.

[16] The relatively large HO_x source from CH_3OOH photolysis stands in sharp contrast to the much smaller source from H_2O_2 photolysis. The contrast can be seen more clearly in the comparison of observed and simulated peroxide concentrations. Figure 5 compares observed and simulated H_2O_2 monthly median profiles at mid and high latitudes. Simulated H_2O_2 concentrations are a factor of $2–10$ higher than the observations; the overestimates increase with decreasing altitude. In comparison, Figure 6 shows that simulated CH_3OOH concentrations are generally in agreement with the observations. Using the rate constant of the HO_2 self reaction suggested recently by *Christensen et al.* [2002], we find that simulated H_2O_2 concentrations decrease by $20–30\%$ at $6–8$ km and $5–15\%$ at $0–4$ km; the large model overestimates remain. The new rate constant has little effects on simulated OH and HO_2 concentrations.

[17] The measurement-model agreement of CH_3OOH at midlatitudes is, however, not as good as those found in the tropics [*Wang et al.*, 2000, 2001]. Particularly noteworthy is that simulated CH_3OOH profiles have a consistent tendency of decreasing with altitude, which is in accordance with the observed profiles of RO_2 concentrations (Figure 3). The observed CH_3OOH profiles, however, show this altitude
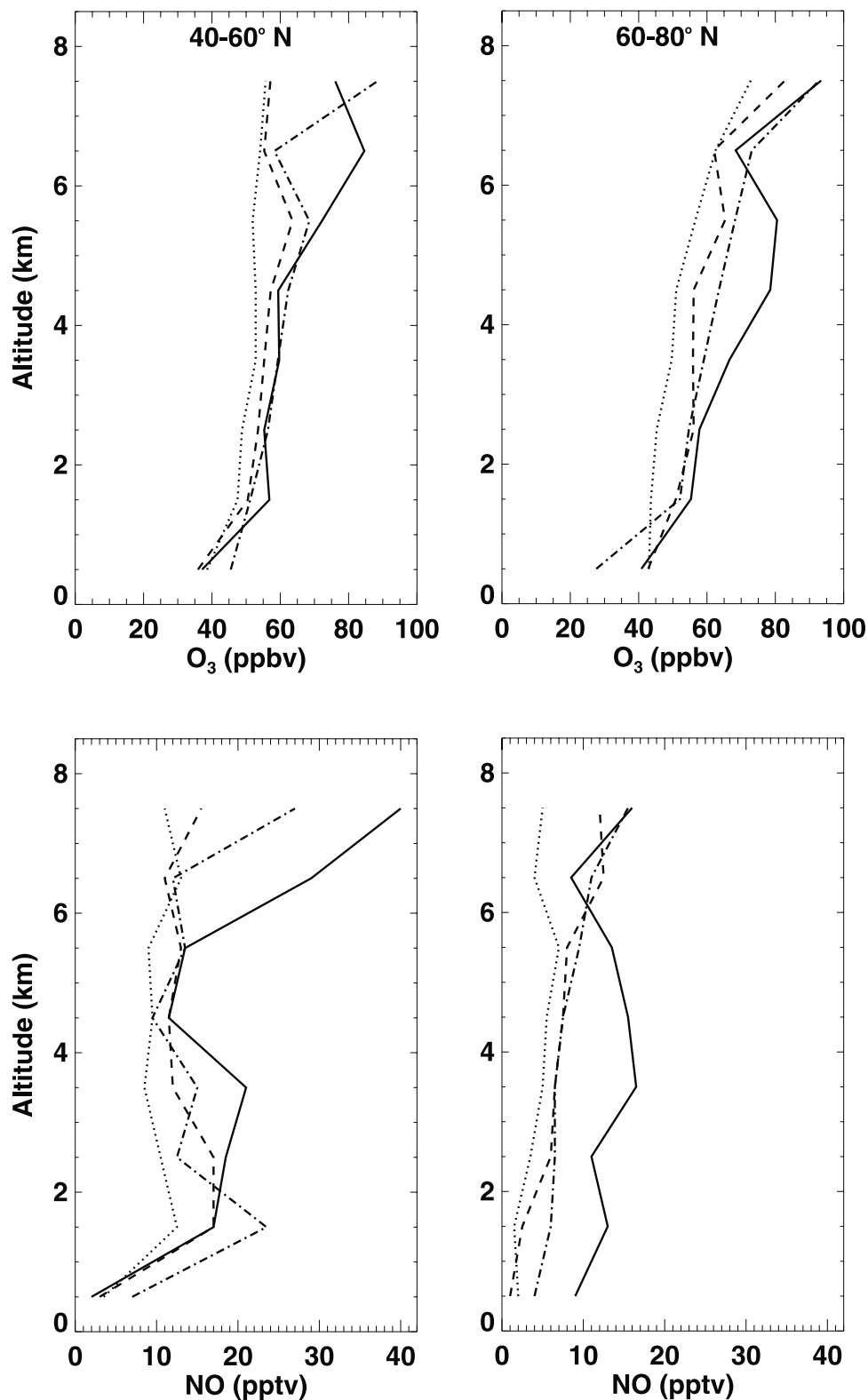
Figure 1. Monthly median profiles of observed O_3, NO, C_2H_2, and CO concentrations at mid (40°– 60°N) and high latitudes (60°–80°N). Data are binned vertically in 1-km intervals. A median value plotted represents a minimum of 10 data points.

dependence in some months but not in others. In particular, the observed profile at midlatitudes in March shows increasing concentrations with altitude, opposite to the trend simulated in the model, resulting in large discrepancies

between observed and simulated values. The model underestimate at 5–8 km is particularly large considering that the model overestimates peroxy radical concentrations in that month (Figure 3). The photochemical lifetime of CH_3OOH
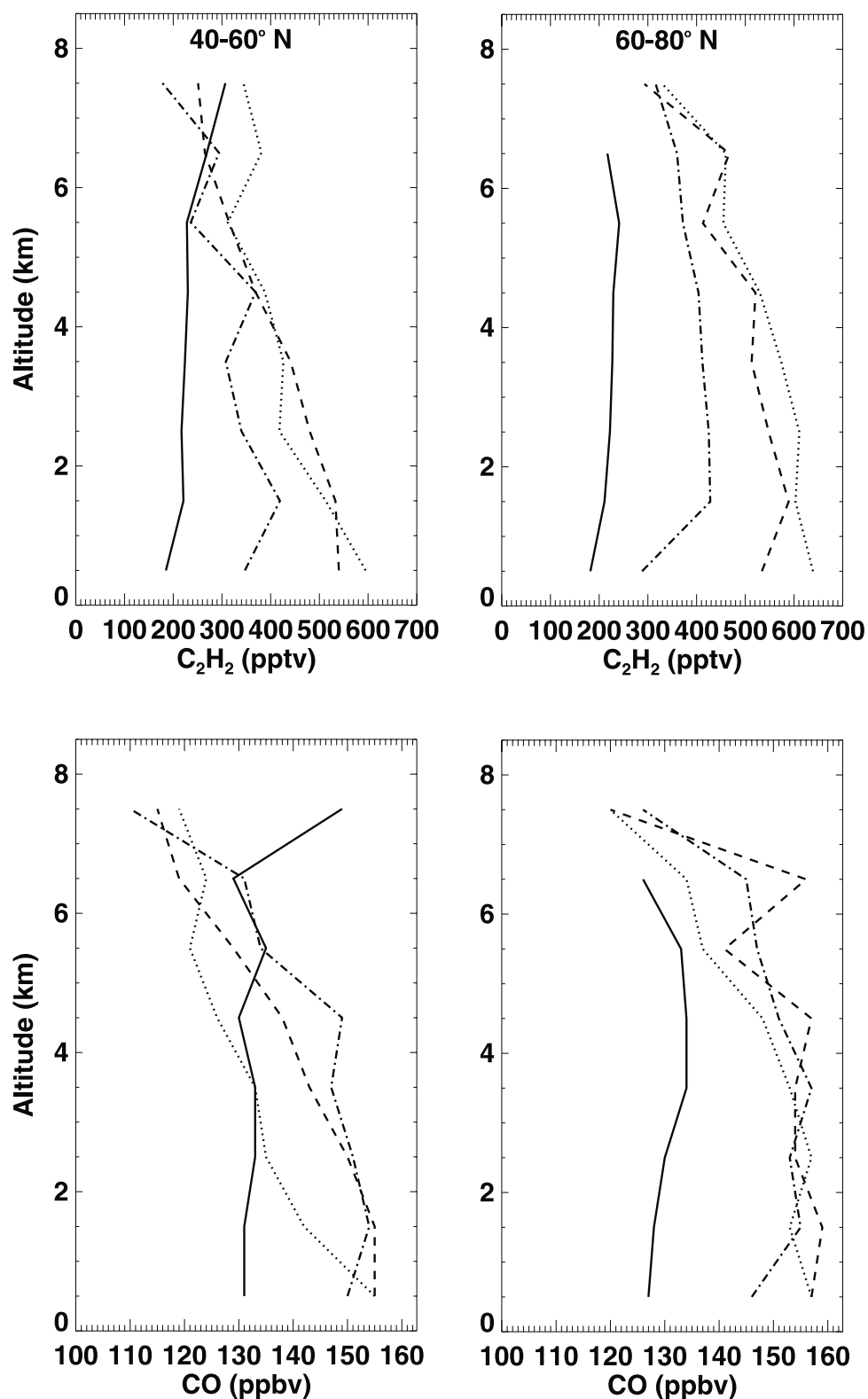
Figure 1. (continued)

is generally several weeks or longer during TOPSE. We examined the 10-day backtrajectories (courtesy of A. Wimmers and J. Moody). Above 4 km, the general flow is controlled by strong westerlies. Some enhancements of CH_3OOH are possible in the upper troposphere due to vertical transport in the upstream regions [e.g., *Prather and Jacob*, 1997]. *Wang et al.* [2001] estimated that the convective enhancement of CH_3OOH over the tropical Pacific during PEM-Tropics B is only 50–150 pptv (above 10 km) despite the short convective turnover timescale of 10 days.
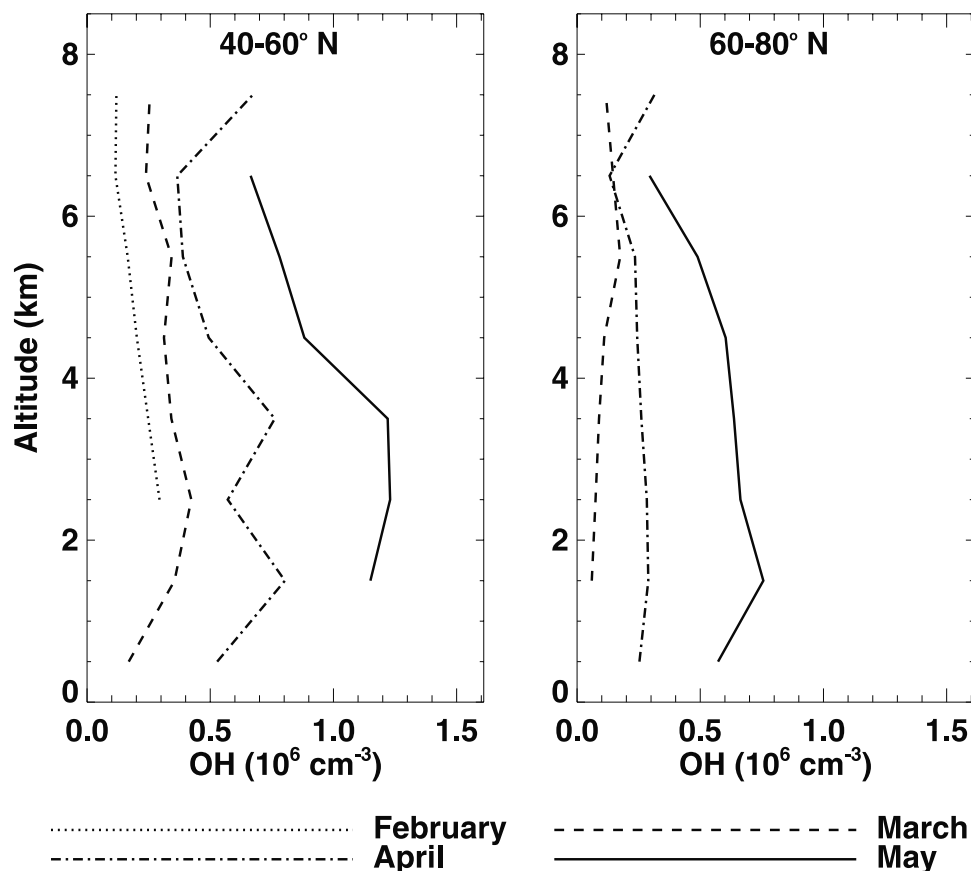
Figure 2. Same as Figure 1 but for simulated 24-hour average OH concentrations at mid and high latitudes. The model was constrained by observed peroxide concentrations.

The concentration of CH_3OOH in the tropical marine boundary is about 1 ppbv. In that work, concentrations of CH_3OOH are lowered by up to 100 pptv at 4–7 km due in part to the subsidence of lower concentrations from higher altitudes. Considering that boundary layer CH_3OOH concentrations in the TOPSE region are only 200–300 pptv, the likely source for high CH_3OOH air masses to the region is from convective transport over the Pacific. The backtrajectory analysis shows, however, flow patterns in April and May similar to that in March. We also examined other chemical tracers but did not find clear signals implicating strong influence by marine air masses in March. The overestimates at 0–4 km may reflect peroxy radical depletion by fresh NO emissions in the upstreamflow from western United States and Canada. A chemistry and transport model will be necessary to explore further the causes for the observed vertical trend of CH_3OOH at midlatitudes in March.

[18] At first glance, the large overestimates of H_2O_2 concentrations but not CH_3OOH might be due to wet scavenging, which efficiently removes soluble H_2O_2 but not CH_3OOH. *Wang et al.* [2001] showed convective scavenging over the tropical Pacific decreases H_2O_2 concentrations by about 30%. Estimating the magnitude of wet scavenging on the basis of meteorological measurements during TOPSE is difficult. Instead we compare the degree of heterogeneous loss of two soluble tracers, H_2O_2 and HNO_3. Concentrations of HNO_3 are also overestimated in the model (not shown). Figure 7 shows the seasonal progression of photochemical

lifetimes of the two species through the spring at mid and high latitudes. The photochemical lifetimes are getting shorter into the summer because of increasing photochemical activity. The photochemical lifetime of HNO_3 is generally about a factor 10 longer than H_2O_2. Furthermore, the solubility of HNO_3 is higher than H_2O_2, making HNO_3 concentrations more sensitive to wet scavenging and deposition loss.

[19] Assuming gas phase oxidation (by OH), photolysis, and scavenging are the pathways for removal of H_2O_2 and HNO_3, we calculate the scavenging timescales necessary to match the observed concentrations in the model (Figure 8). The required timescales for HNO_3 scavenging are consistent with known rainout frequency and high solubility of HNO_3. The required scavenging is much faster at midlatitudes than at high latitudes, reflecting more frequent rainout at midlatitudes. The general trend of decreasing scavenging with altitude is also consistent with the distribution of rainout. The timescales of HNO_3 against scavenging loss are about 1 week at midlatitudes and 2–4 weeks at high latitudes. Our estimates of HNO_3 scavenging timescale are likely the upper limits since we do not take into account the heterogeneous production of HNO_3 by N_2O_5 hydrolysis on aerosols, which could be significant particularly at midlatitudes [*Tie et al.*, 2002]. Nonetheless, the derived timescales are in line with the estimates derived from a global 3-D study of the observed ^{210}Pb distributions by *Balkanski et al.* [1993].

[20] The required timescales of H_2O_2 scavenging are more difficult to understand. First, the required scavenging
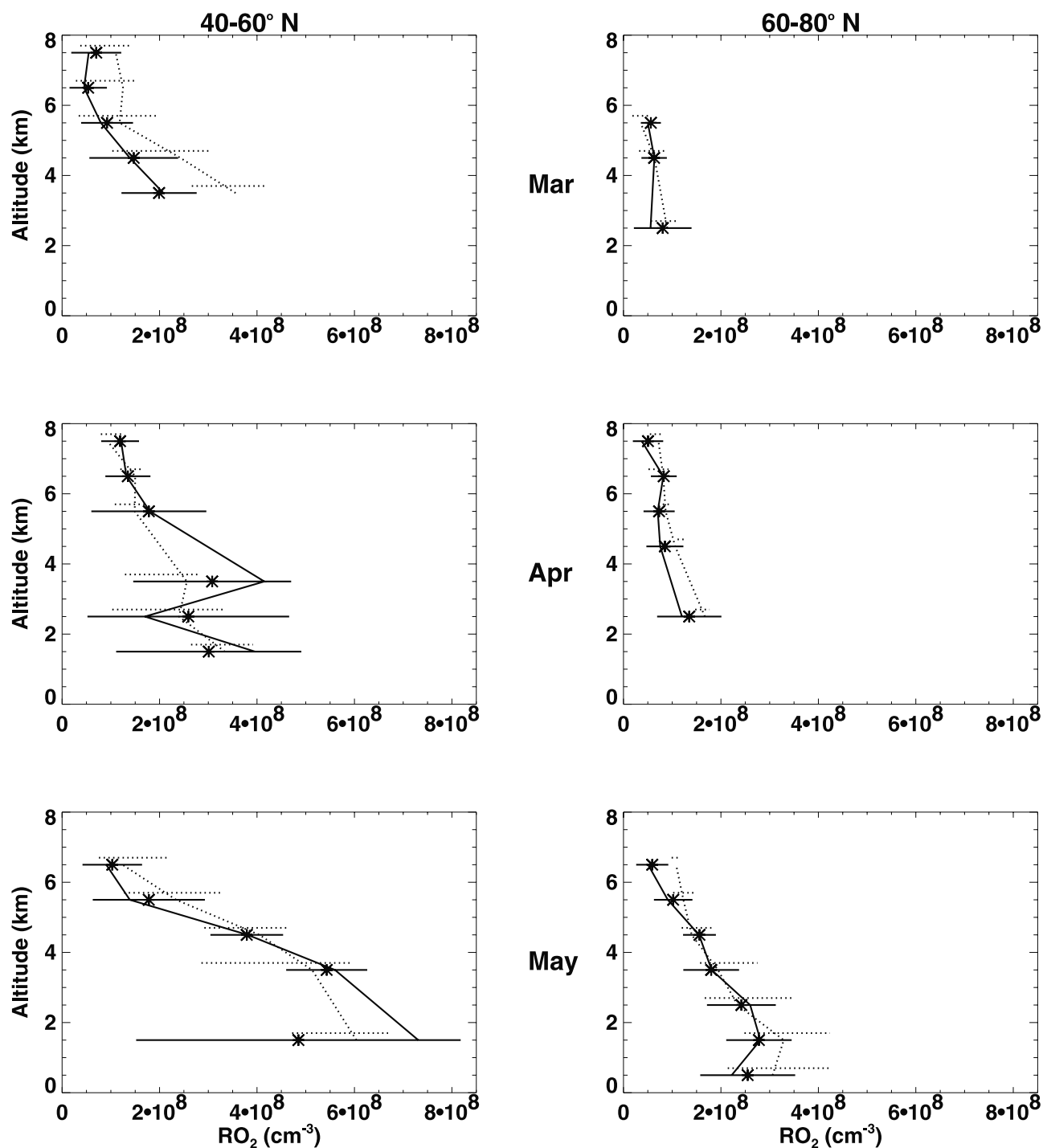
Figure 3. Monthly median profiles of observed and simulated total peroxy radicals (RO$_2$) at mid and high latitudes. The solid vertical lines show the observed medians in 1-km intervals. The solid horizontal lines and asterisks are the observed standard deviations and means, respectively. Simulated medians and standard deviations are shown in dashed lines. Model calculations are constrained by observed peroxide concentrations. Each observation data point has a corresponding simulated value and vice versa. A median value plotted represents a minimum of 10 data points. Not enough data are available for February.

frequency of H$_2$O$_2$ is up to a factor of 10 faster than that of HNO$_3$. In May, the loss by scavenging is about half a day at midlatitudes and 1 day at high latitudes. Second, the required scavenging frequency of H$_2$O$_2$ is more seasonal than that of HNO$_3$. The seasonal increase of the former is about a factor of 5 at mid and high latitudes. In contrast, the scavenging frequency of HNO$_3$ shows no clear seasonal change at midlatitudes and a much smaller increase (mostly
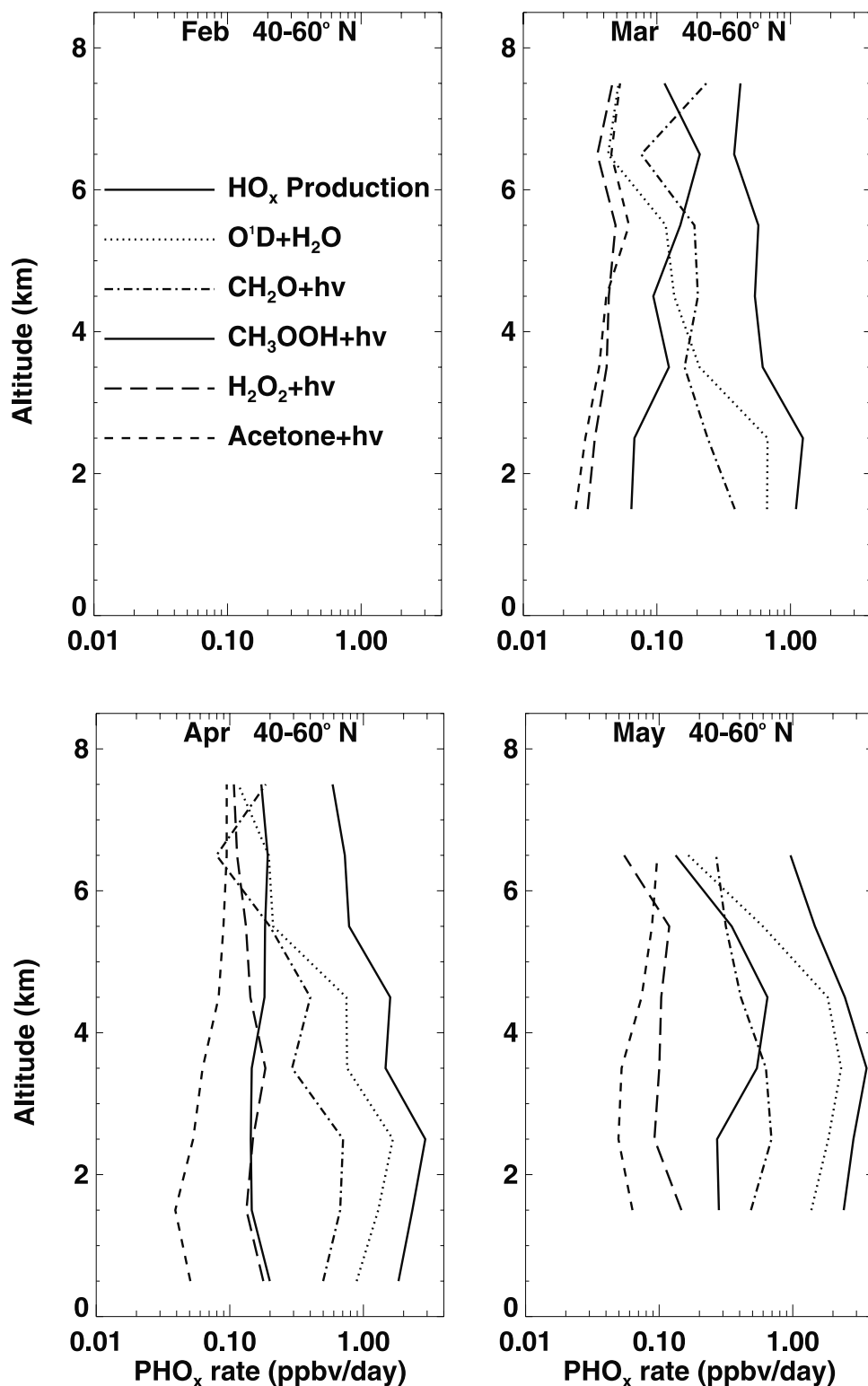
Figure 4.   Same as Figure 1 but for simulated 24-hour average HO_x sources. The model is constrained with observed peroxide and CH_2O concentrations. The HO_x yield of CH_2O photolysis is computed on line.

from April to May) at high latitudes. Simple rainout that applies both to HNO_3 and H_2O_2 cannot explain the different characteristics in the required scavenging frequencies of the two species and the rapid rates of H_2O_2 removal at mid-

latitudes. Similar results for H_2O_2 scavenging are obtained when using the rate constant of the HO_2 self reaction recommended by *Christensen et al.* [2002]. One possible pathway is heterogeneous removal of H_2O_2 by SO_2 oxida-
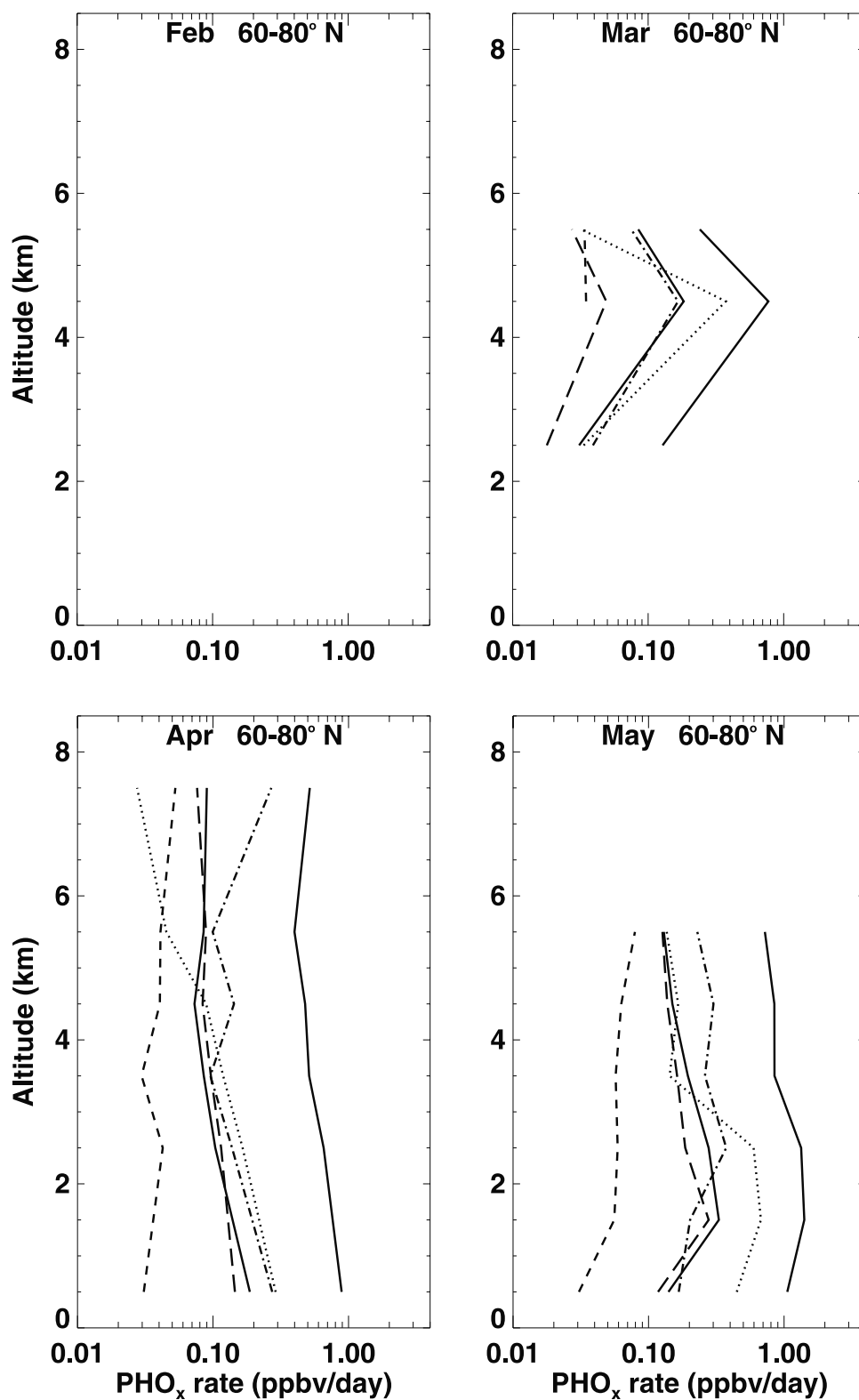
Figure 4. (continued)

tion in droplets [e.g., *Hoffmann and Edwards*, 1975]. The observed monthly median profiles of SO_2 concentrations (not shown) peak in February and are lowest in May. The concentrations are generally in the range of 10–60 pptv, which are too low to account for significant H_2O_2 loss.

Furthermore, considering that the average photochemical steady state concentrations of H_2O_2 are >1 ppbv at mid-latitudes from March to May and that the required scavenging lifetime is <1 day, the supply of SO_2 to the TOPSE region needs to be >1 ppbv/day. In terms of the sulfur
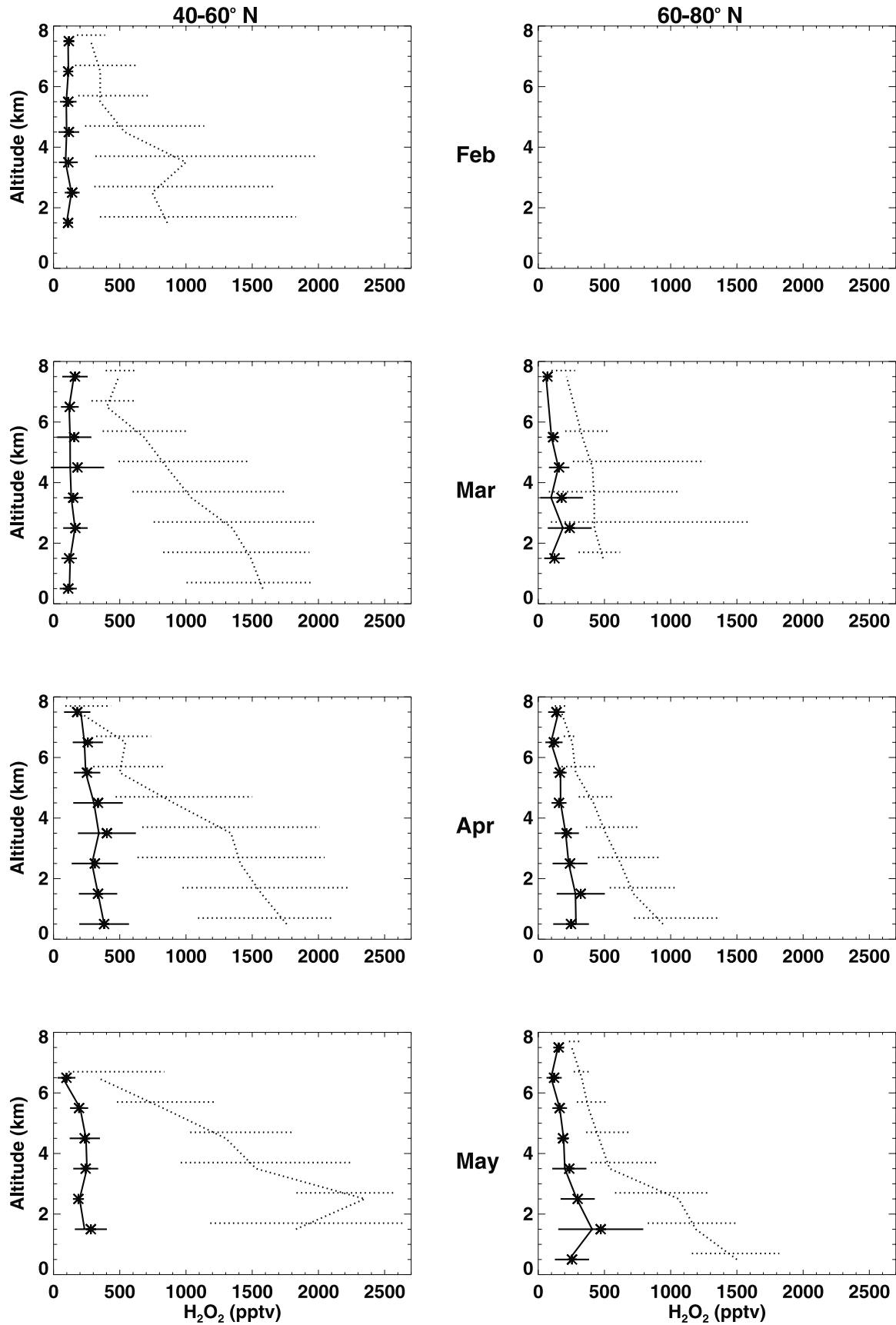
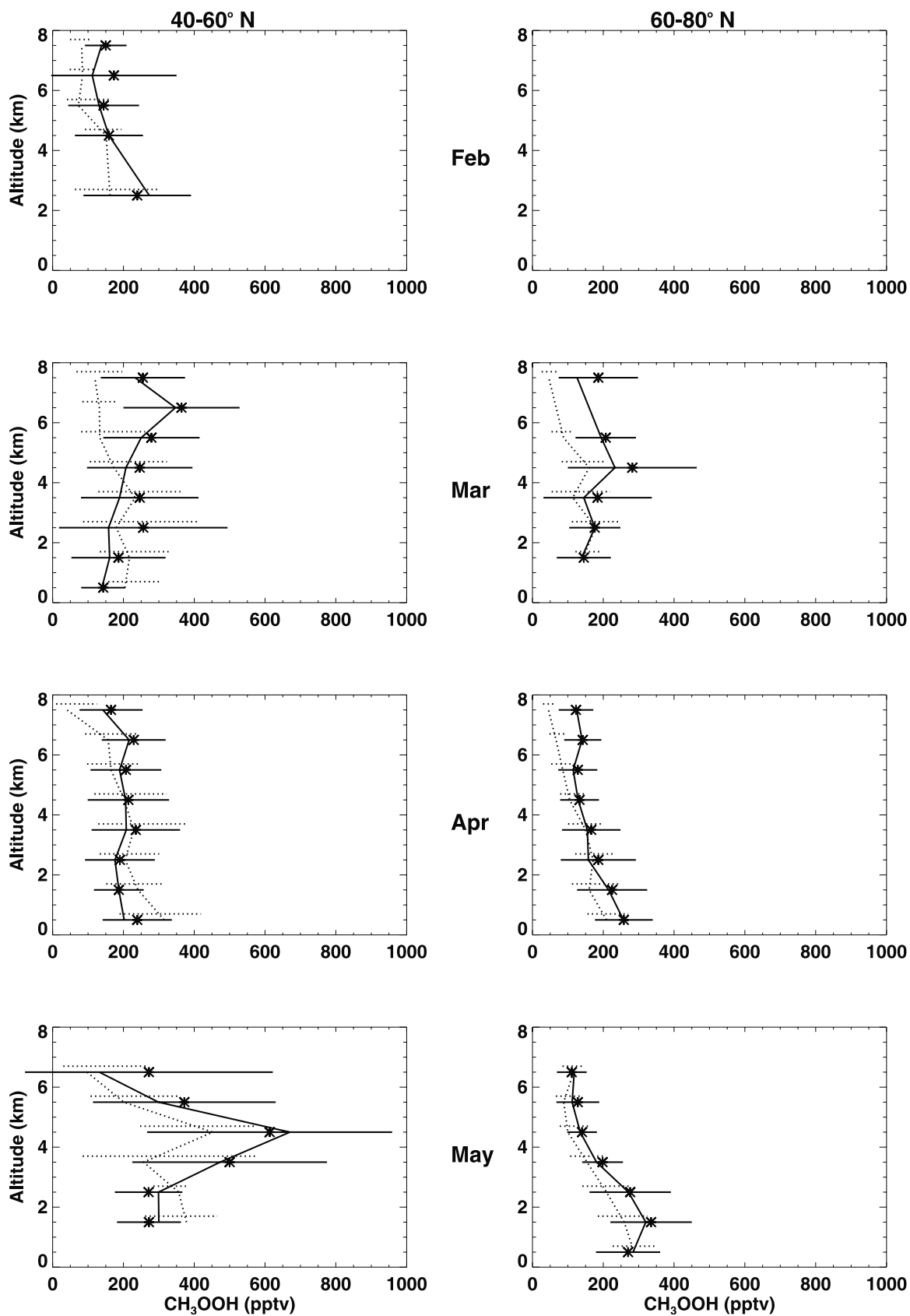**Figure 5.**   Same as Figure 3 but for H_2O_2. The model is not constrained by observed peroxides.

Figure 6. Same as Figure 3 but for CH_3OOH. The model is constrained by observed H_2O_2 concentrations.
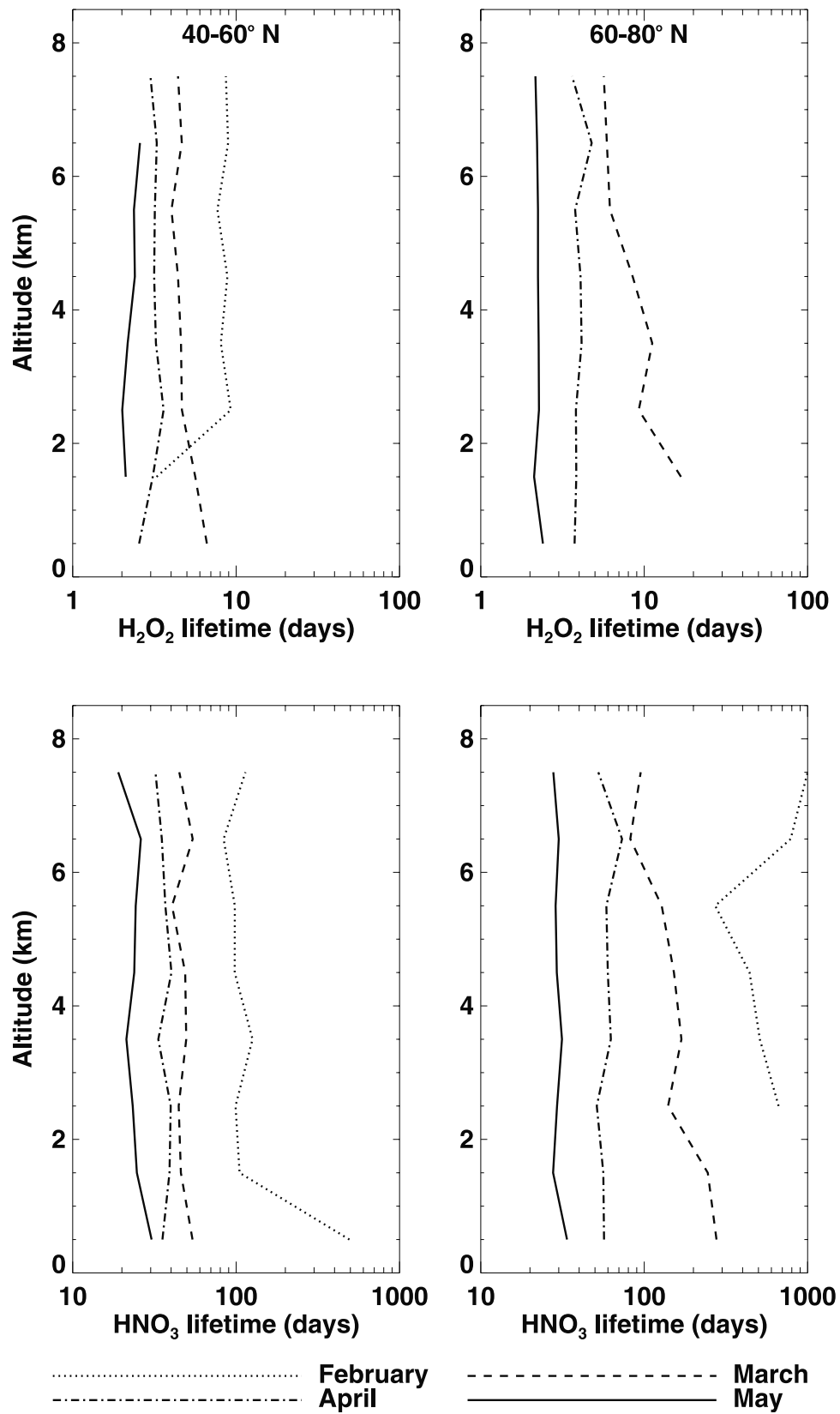
Figure 7.   Same as Figure 1 but for simulated photochemical lifetimes of H_2O_2 and HNO_3.
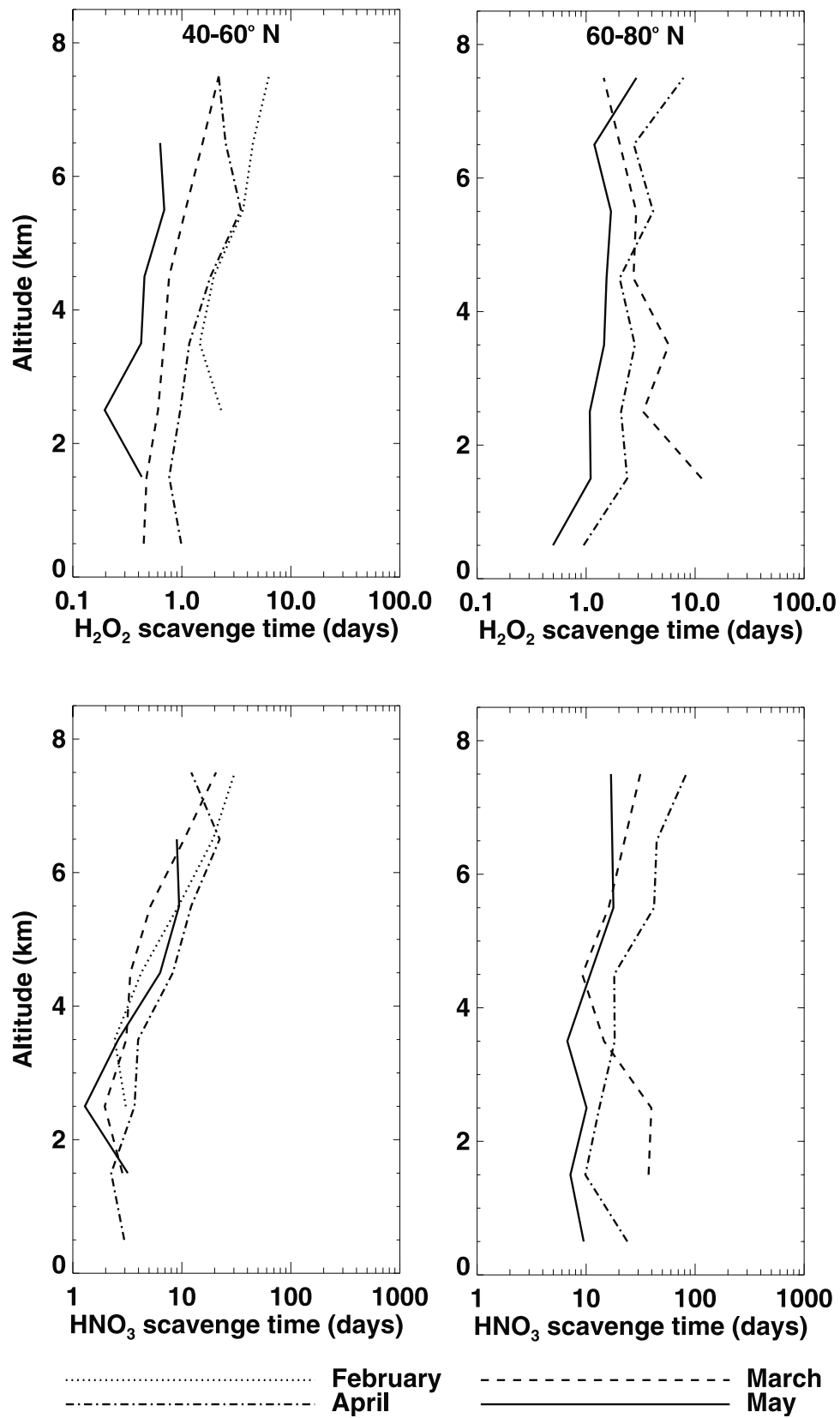
Figure 8. Same as Figure 1 but for estimated scavenging timescales of H_2O_2 and HNO_3 necessary to explain the observed concentrations.

budget, it implies a SO_4^{2-} wet deposition rate for the TOPSE region of >2.5 g S m^{-2} yr^{-1}, a rate more than 1 order of magnitude larger than estimated by *Langer and Rodhe* [1991]. Other SO_2 like compounds are necessary to explain the derived scavenging rates.

[21] A survey of previous comparisons of simulated and observed H_2O_2 concentrations suggests that the rapid scavenging loss required for TOPSE observations is unique. The box models used in the analyses cited below are similar to the one used in this study and H_2O_2 was measured in a similar manner in those field experiments as during TOPSE. *Davis et al.* [1996] showed relatively good agreement between simulated and observed H_2O_2 during PEM-West A over the western Pacific (September–October). Heterogeneous removal of H_2O_2 was assumed in that model to have a timescale of 5 days below 4 km and longer at higher altitude. *Jacob et al.* [1996] found that the model could account for most of the observed H_2O_2 at 0–8 km during TRACE-A over the tropical South Atlantic (September–October). *Schultz et al.* [1999] found good simulation-measurement agreement at 2–8 km but the model was too high by a factor of 2 at 0–2 km during PEM-tropics A over the tropical Pacific (August–September). *Jaeglé et al.* [2000] showed reasonable agreement between simulated and observed H_2O_2 during SONEX over the North Atlantic (October–November). Unlike in the work by *Davis et al.* [1996], no heterogeneous loss of H_2O_2 was included in the other three works. The latter two studies included heterogeneous production of H_2O_2 from HO_2 on aerosols. The rate of heterogeneous production used by *Schultz et al.* [1999] is H_2O dependent with a γ of 0.1 whereas that by *Jaeglé et al.* [2000] depended only on HO_2 and aerosol surface area with a γ of 0.2. Without the heterogeneous production, model results would be considerably lower than observations in the work by *Jaeglé et al.* [2000]. It is unclear what effects heterogeneous production had in the work by *Schultz et al.* [1999], particularly how much it contributed to the model overestimates at 0–2 km. *Wang et al.* [2000] showed that a 1-D model with a column convective turnover timescale of 20 days could largely reproduce the observed profile of H_2O_2 during PEM-Tropics A.

[22] The required scavenging loss of H_2O_2 implies rapid removal of a large reservoir of HO_x and consequently slows down the HO_x cycles and O_3 production. Figure 9 shows the ratios of 24-hour average HO_x production, OH concentrations, and O_3 production in the simulations using observed versus simulated H_2O_2 concentrations. The relative effects are similar at mid and high latitudes and among different months. The decrease of HO_x source from the photolysis of H_2O_2 leads to a loss of 20–40% in the production of HO_x. The decrease of 20–30% in OH concentrations is larger than that of 10–20% for the peroxy radicals (not shown), which results in a similar decrease in O_3 production. The photochemical loss (and hence the net production or loss) also decreases in a similar proportion, reflecting the importance of the reaction of O_3 and HO_2 in O_3 loss (section 5).

3.2. CH_2O as a Large Source of HO_x at Northern High Latitudes

[23] Among the HO_x sources shown in Figure 4, the photolysis of CH_2O is particularly large. Relative to the total HO_x source, it is larger at higher altitudes and latitudes

where the decrease of H_2O vapor concentrations with temperature reduces the source from the reaction of $O(^1D)$ and H_2O. This HO_x source often reflects the auto-catalytic nature of the HO_x cycles since CH_2O is largely produced during the OH oxidation of hydrocarbons.

[24] However, standard gas-phase photochemistry alone cannot explain the observed CH_2O concentrations at high altitudes in northern high latitudes, where CH_2O photolysis is of great importance to the HO_x budget. Figure 10 compares model simulated median profiles of CH_2O with observations. Simulated median CH_2O concentrations are generally within the standard deviation of the observed concentrations. Whereas good agreement was found for midlatitude observations, simulated CH_2O concentrations were much lower at high latitudes in March. These underestimates are particularly large at higher altitudes. *Fried et al.* [2002] further examined the model underestimates and investigated a number of possibilities that could increase CH_2O production at high latitudes and altitudes, including direct production from the reaction of CH_3O_2 and HO_2 [*Ayers et al.*, 1997], the decomposition of CH_3OONO_2 [*Cantrell et al.*, 2002], and heterogeneous conversion of CH_3OH to CH_2O in aerosols [*Singh et al.*, 2000]. They found no clear evidence attributing the observed excess CH_2O to these pathways. Another hypothesis is mixing between mid and high latitude air masses enhances CH_2O concentrations at high latitudes.

[25] Simulated CH_2O concentrations are affected by CH_3OOH concentrations [*Liu et al.*, 1992]. The sensitivity varies. The model underestimates at high altitudes are larger when model simulated CH_3OOH concentrations are used instead of observed CH_3OOH (Figure 11). The effect is particularly large at 6–8 km in March; using observed in place of simulated CH_3OOH concentrations in the model increases CH_2O concentrations by about 50–100% (20–30 pptv). In general, the enhancements are above 4 km; the increase is about 10–40% in April and May. The assumption used to calculate acetone concentrations by scaling to CO concentrations is another factor contributing to the uncertainty in the simulated CH_2O concentrations. *Jacob et al.* [2002] suggested that acetone concentrations are lower in winter and spring than in the fall due to the loss of acetone to the oceans. Reducing our estimated acetone concentrations by half matches the levels (300–600 ppbv) simulated by *Jacob et al.* [2002] for North America in January. The lowering of acetone concentrations decreases simulated CH_2O concentrations by 10–20% above 5 km, which will increase the underestimates by the model.

[26] It is unclear if the additional CH_2O beyond the level that can be sustained by the standard gas-phase photochemistry is a primary or secondary source of HO_x at high altitudes since the nature of the model underestimate is unknown. However, we can examine the various hypotheses more closely. If the additional CH_2O is due to transport or conversion of CH_3OH in aerosols, its photolysis increases the primary HO_x source. If it is due to production from the reaction of CH_3O_2 and HO_2 or from CH_3OONO_2 decomposition, the additional HO_x source is secondary. Boosting the secondary HO_x source implies more efficient yields of CH_2O from hydrocarbon oxidation. Considering that CH_4 oxidation provides about 70–80% of the total CH_2O source
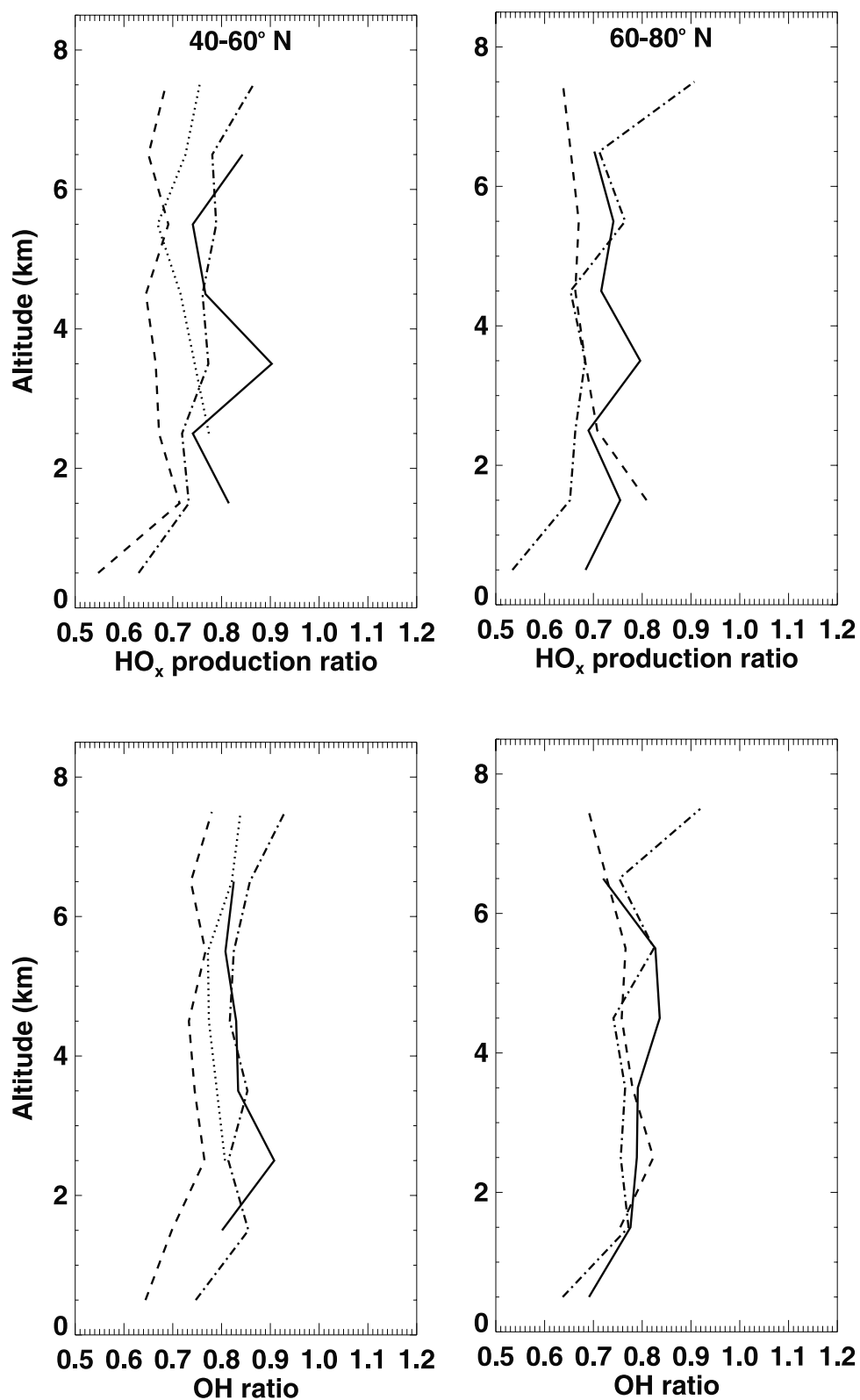
Figure 9. The monthly median ratios of simulated 24-hour average HO_x production, OH concentrations, and O_3 production with relative to without constraining H_2O_2 to the observed values in the model. A median value plotted represents a minimum of 10 data points.
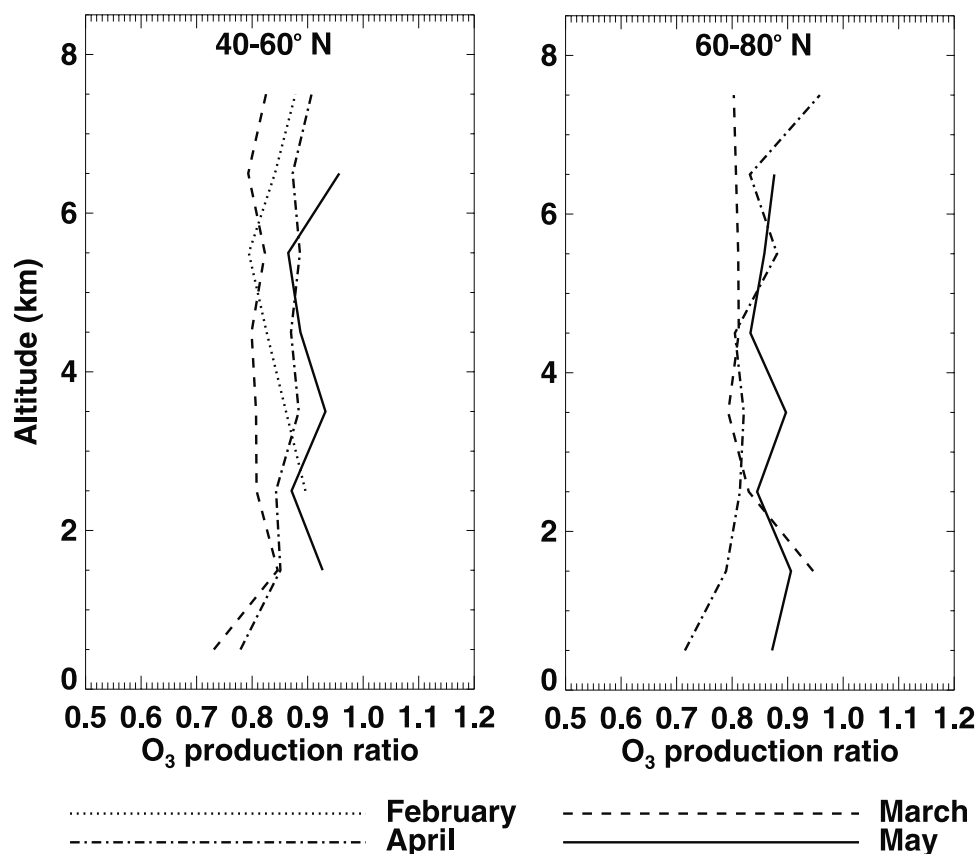
Figure 9. (continued)

and that the yield of CH$_2$O from this oxidation is already close to 1 in the box model (with no heterogeneous loss of CH$_3$OOH assumed), it is unlikely that these pathways will significantly increase CH$_2$O concentrations to make up for the large underestimates shown in Figure 10. Therefore, it is more likely that the additional HO$_x$ source from CH$_2$O photolysis is primary.

[27] Figure 12 shows the ratios of 24-hour average HO$_x$ production, OH concentrations, and O$_3$ production in the simulations using observed versus simulated CH$_2$O concentrations. The effects are significant at high latitudes above 6 km and are larger in March than in May. The largest effect is seen in the total production of HO$_x$, decreasing from a factor of 2 to 30% from March to May above 6 km at high latitudes. In the region, the concentrations of OH and HO$_2$ (not shown) and the production of O$_3$ increase by 20–50%. The seasonal decrease in the relative contribution of the "excess" CH$_2$O to HO$_x$ reflects in part the increasing contribution from the reaction O(^{1}D) and H$_2$O to the HO$_x$ source with time and in part lesser underestimates by the model in late spring [*Fried et al.*, 2002]. The effects are minimal at midlatitudes where simulated and observed CH$_2$O concentrations are in better agreement. Photolysis of acetone also affects HO$_x$ chemistry at high altitudes [e.g., *McKeen et al.*, 1997]. During the TOPSE period, it is not the dominant HO$_x$ sources (Figure 4). Reducing acetone concentrations estimated in the model by half decreases HO$_x$ production by up to 12 and 20% at mid and high latitudes (>6 km), respectively. The effects on the concentration of OH and O$_3$ production are around 10% at altitude

above 6 km. The effects are insignificant below 4 km where the source from the reaction of O(^{1}D) and H$_2$O dominates HO$_x$ production.

4. Nitrogen Oxides and In Situ O$_3$ Production

[28] Figure 13 compares simulated and observed monthly median profiles of NO$_2$ at mid and high latitudes. Although the simulated median profiles of NO$_2$ at given altitude bins are within the observed monthly standard deviations, which are often larger than the scale of the plots and are hence not shown, simulated NO$_2$ concentrations tend to be lower than the observations. The underestimates are largest above 6 km (about 10 pptv). Some of the discrepancies can be attributed to the measurement uncertainty, which increases with altitude from 3 pptv to 8 pptv. The increasing measurement uncertainties with altitude are also reflected in the increasing proportion of data near the detection limits, reaching 50% at 6–8 km. The model overestimate at 1–2 km in February at midlatitudes is due to some high concentration plumes sampled by the C-130. On the basis of observed NO concentrations, the model predicts broader plumes than found in the NO$_2$ measurements. When model points with no corresponding NO$_2$ measurements are included, the median model value drops to 25 pptv and is in agreement with the observations. The seasonal increase of NO concentrations during TOPSE is shown in Figure 1. In comparison, the seasonal increase of NO$_2$ is much smaller, reflecting the shift of NO$_x$ partition toward NO as photolysis of NO$_2$ increases with time.
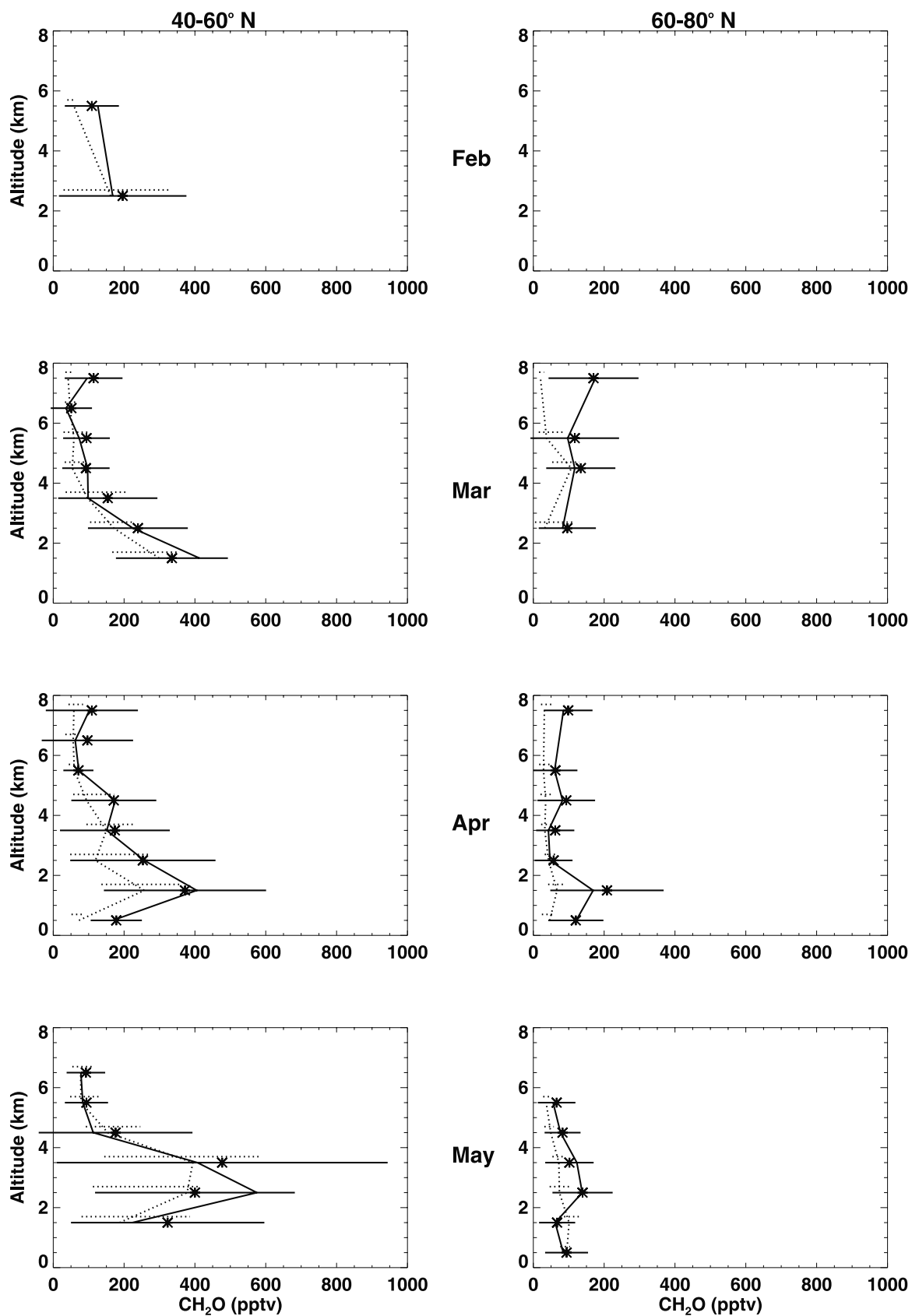
Figure 10. Same as Figure 3 but for CH_2O. A median value plotted represents a minimum of 5 data points.
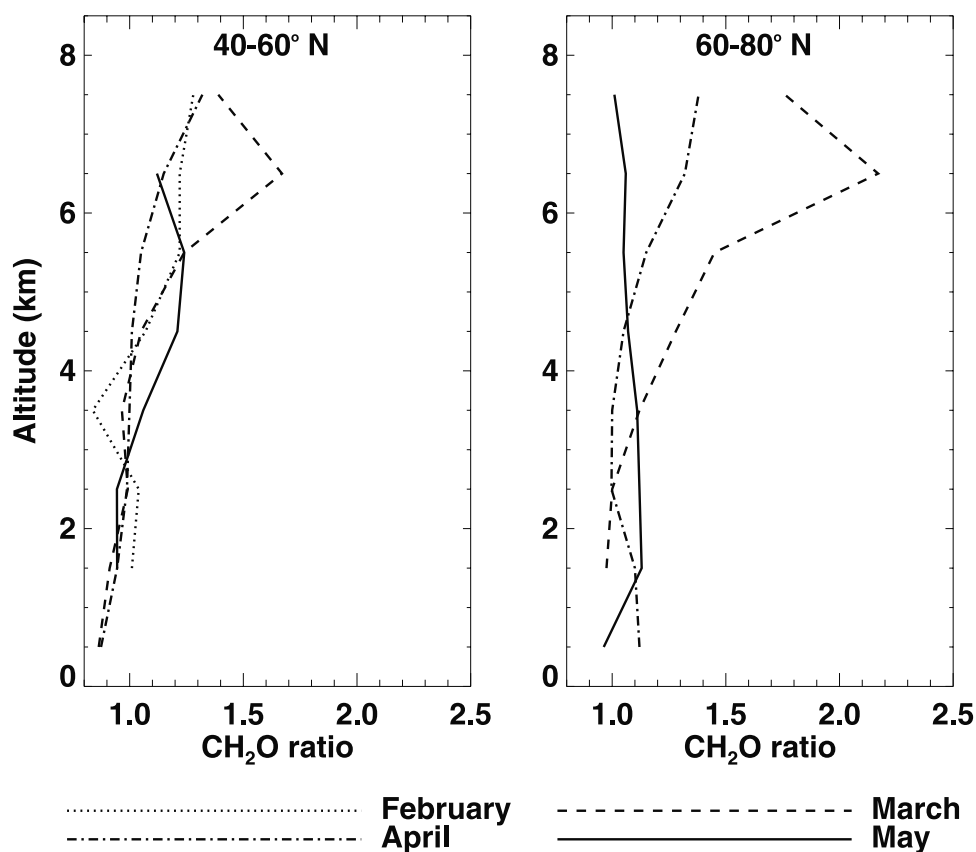
Figure 11. The monthly median ratios of simulated CH_2O concentrations with relative to without constraining CH_3OOH to observed values in the model. Each median value represents a minimum of 5 data points. The model is constrained by observed H_2O_2 concentrations.

[29] *Jaeglé et al.* [1999] mapped O_3 production as a function of the primary source of HO_x and NO_x concentration for the observations during SONEX. Figure 14 shows the mapping for TOPSE observations, where the primary HO_x source is driven mostly by the reaction of $O(^1D)$ and H_2O. Compared with SONEX, two features stand out. First, there is a clear positive correlation between primary HO_x production and NO_x concentrations, whereas *Jaeglé et al.* [1999] found marine convected air masses (over the North Atlantic) with high primary HO_x production but low NO_x concentrations during SONEX. During TOPSE, the positive correlation reflects the convergence of favorable photochemical environment (Figure 4) and increasing NO_x concentrations. Second, in the same range of primary HO_x production rates and NO_x concentrations, the O_3 production rates are similar between TOPSE and SONEX despite that our work is for 0–8 km in spring and the work by *Jaeglé et al.* [1999] is for 8–12 km in the fall.

[30] A casual look of the first panel of Figure 14 would suggest that the primary HO_x production does not play a significant role in the production rate of O_3. Part of the insensitivity of O_3 production to the primary HO_x source is due to the rapid increase of NO/NO_2 ratio with altitude, which is driven by the temperature dependence of the NO + O_3 reaction and the altitude dependence of air density and photon flux. The same amount of NO_x is therefore more effective in O_3 production at high altitudes where NO/NO_2 ratio is high since the production is driven by the reaction of

NO with peroxy radicals. This effect combined with a decreasing trend of the HO_x primary production with altitude tends to mask the contribution of the primary HO_x source to O_3 production.

[31] We therefore mapped O_3 production as a function of NO in Figure 14 as well. At NO levels above 10 pptv, it is clear that increasing the primary HO_x source enhances O_3 production. Considering that the range of the primary HO_x source spans about 4 orders of magnitudes, the efficiency of primary HO_x production in boosting O_3 production ($\partial P(O_3)/\partial P(HO_x)$) is less than that of NO_x (or NO). However, it should be noted that the increase of primary HO_x production through the spring is much more rapid than that of NO (Figures 1 and 4). The large dependence of O_3 production on NO concentrations reflects a NO_x-limited photochemical regime during TOPSE.

5. Budgets of Reactive Nitrogen and O_3

[32] *Penkett and Brice* [1986] used the rapid buildup and loss of peroxyacetylnitrate (PAN) at a rural site in spring as a proxy to suggest that intensifying photochemistry activity contributes to the observed springtime O_3 maximum. *Honrath et al.* [1996] further suggested that the accumulation of reactive nitrogen at winter high latitudes and the subsequent decomposition of these reservoirs back to NO_x in spring could contribute to the observed springtime maximum.
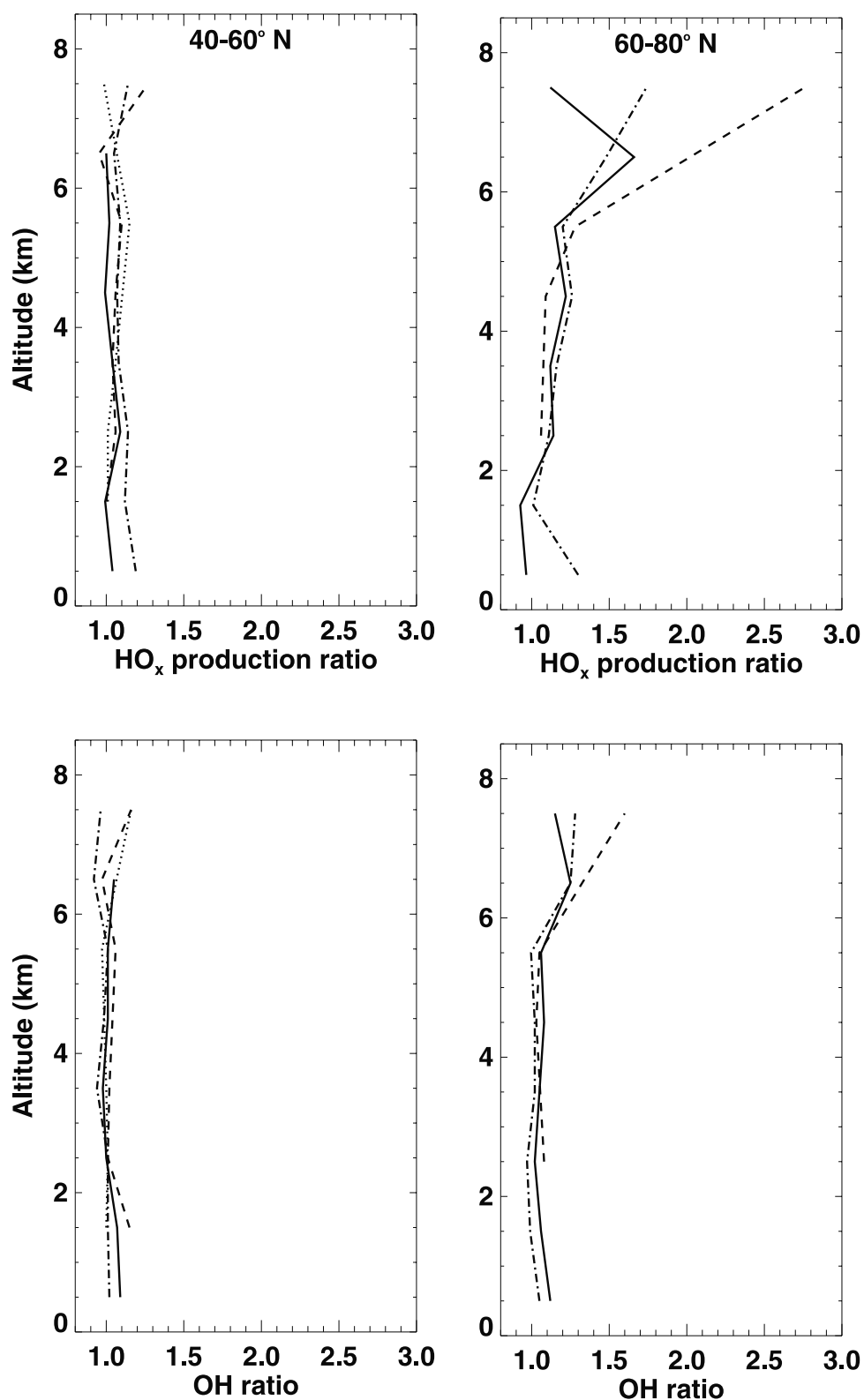
Figure 12. The monthly median ratios of simulated 24-hour average HO_x production, OH, and O_3 production with relative to without constraining CH_2O to the observed values in the model. Peroxides in the model are specified as observed. Each median value represents a minimum of 5 data points.

[33] Figure 15 shows the monthly median profiles of total reactive nitrogen (NO_y) and PAN concentrations at mid and high latitudes. The most abundant NO_y component is PAN accounting for 40–80% of NO_y. The PAN fraction in NO_y decreases with season. The continually increasing concentrations of NO_y and PAN in the most part of the troposphere show no evidence for wintertime accumulation at high latitudes followed by springtime transport to midlatitudes.
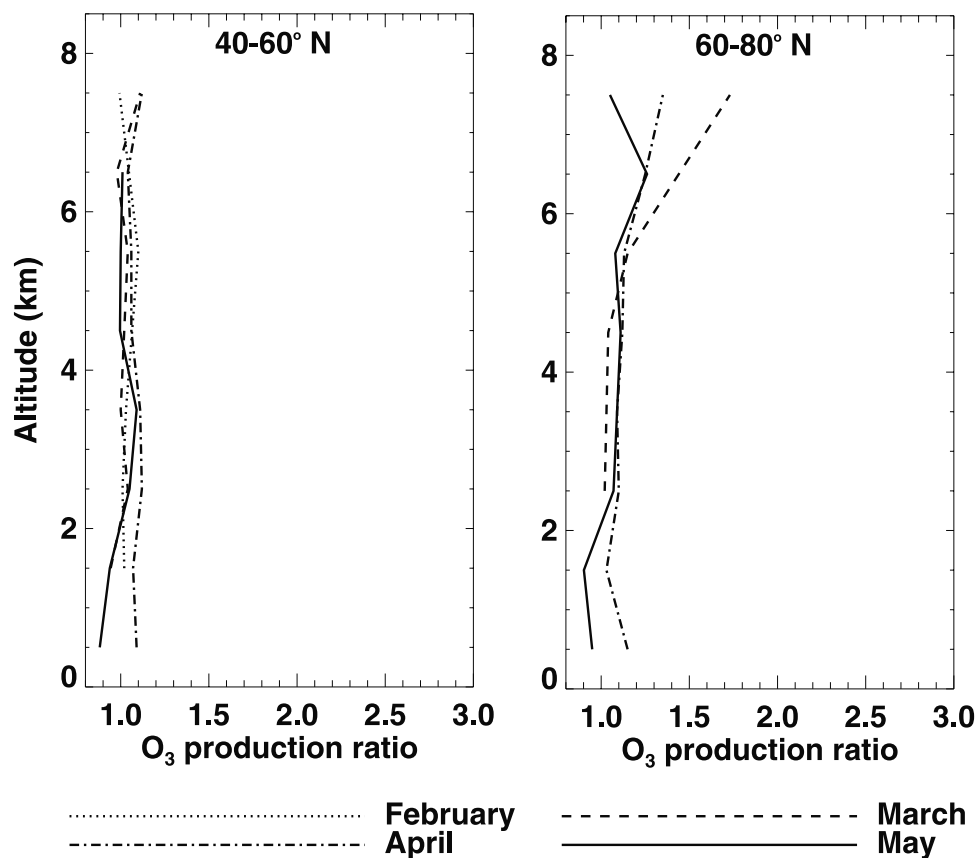
Figure 12.   (continued)

Free tropospheric measurements are particularly important in understanding the seasonality of reactive nitrogen species at mid and high latitudes because the seasonal trends are quite different near the surface from that in the free troposphere. Concentrations of NO_y and PAN above 3 km continue to increase throughout the spring. The seasonal trend at lower altitudes is not as well defined as that at higher altitudes. The concentrations of NO_y tend to peak in February near the surface; the seasonal maximum of PAN near the surface is shifted toward April particularly at midlatitudes.

[34]   The apparent disparity in the observed seasonal variations of NO_y and PAN near the surface would imply that some major component of NO_y decreases throughout the spring as NMHCs (Figure 1), particularly in light of the increasing HNO_3 concentrations with season (not shown). However, no such component is found. To illustrate the point, we show in Figure 15 the seasonal profiles of DNO_y, defined as $NO_y - (NO + NO_2 + PAN + PPN + HNO_3 + 2N_2O_5 + HNO_4)$. Simulated N_2O_5 and HNO_4 are used because these species were not measured. We also used model computed NO_2 concentrations to increase the availability of data points. Unlike in many tropospheric missions [e.g., *Bradshaw et al.*, 2000], there is generally no need to invoke missing nitrogen species to account for measured NO_y concentrations during TOPSE. The exception is in February when NO_y concentrations are higher than the sums of individual components by $50-100$ pptv. We note the extreme scarcity of overlapping reactive nitrogen data in February; the median profiles for that month are generated from $1-3$ points at 1-km intervals. There is an opposite

problem most of the time, i.e., measured NO_y concentrations are not enough to match the sums of reactive nitrogen species. This shortfall from NO_y measurements increases from March to May at both mid and high latitudes. Without counting model simulated HNO_4 concentrations, the shortfall can be largely eliminated at high altitudes but not at lower altitudes, where simulated HNO_4 concentrations are low due to relatively high temperatures. We note that DNO_y carries the uncertainties in the measurements or model simulations of all the components. Detailed analysis of measurement uncertainties is carried out by F. Flocke et al. (The behavior of PAN and the balance of odd nitrogen during TOPSE, submitted to *Journal of Geophysical Research*, 2002). In particular, there is evidence for occasional interference of particulate and cloud nitrates in the HNO_3 measurements (Flocke et al., submitted manuscript, 2002).

[35]   We examine now the budget of reactive nitrogen during the TOPSE experiment. Among the reactive nitrogen reservoirs, PAN and HNO_3 concentrations are largest. Peroxypropionylnitrate is not simulated in the model. Its behavior follows closely that of PAN (Flocke et al., submitted manuscript, 2002); we hence expect its budget resembles that of PAN as well. Figure 16 shows the seasonal evolution of the net production rates for these two species at mid and high latitudes. Loss of NO_x to HNO_3 is likely underestimated particularly at midlatitudes because heterogeneous conversion in aerosols via N_2O_5 hydrolysis is not accounted for in the model. There is a net loss of NO_x to HNO_3 and PAN during TOPSE. The loss to HNO_3 is much more significant at mid than high latitudes because of
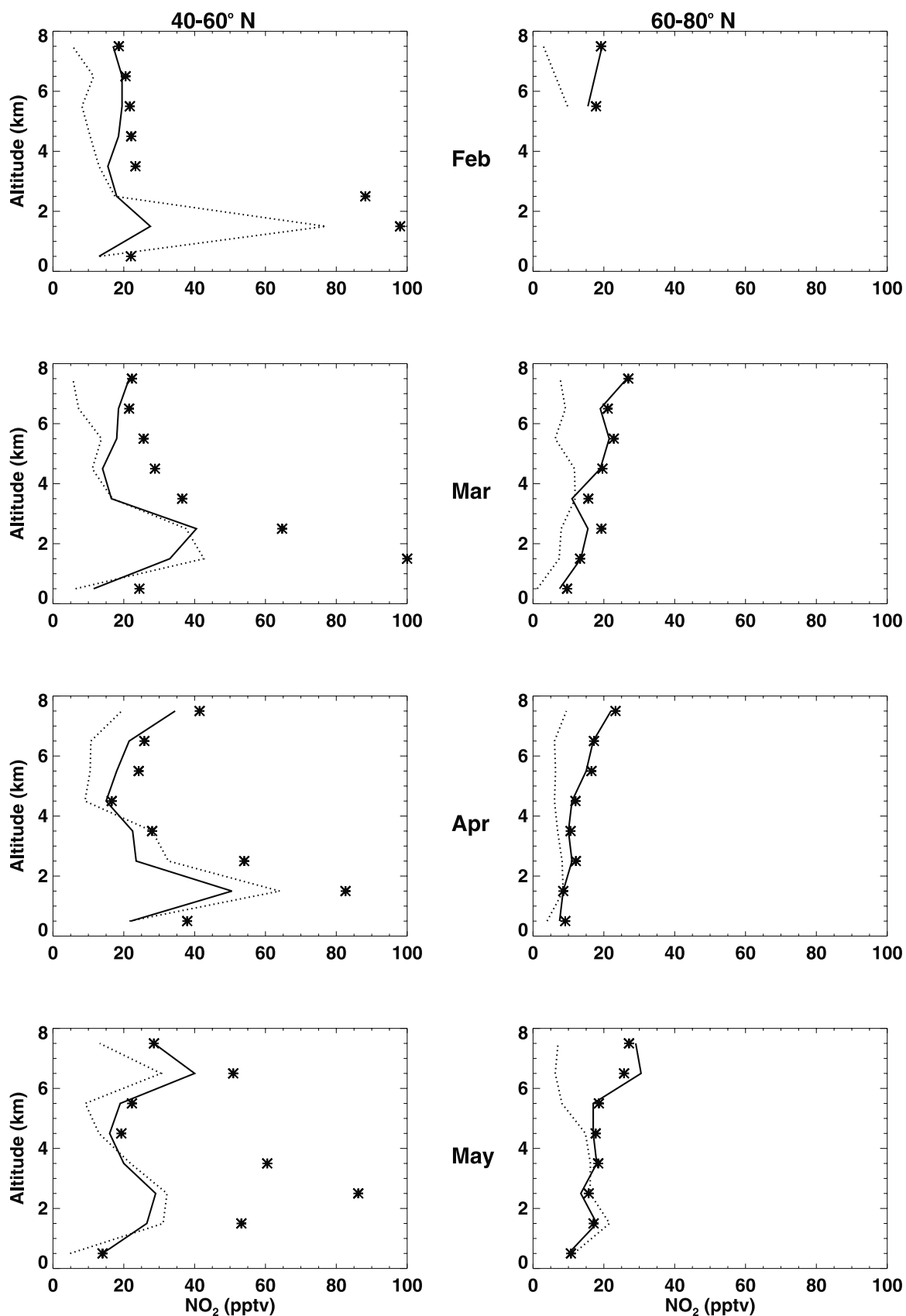
Figure 13. Same as Figure 5 but for NO_2. Line symbols are the same as Figure 3. Standard deviations are not shown because of the large data variability, which is reflected in the large differences between observed means and medians at mid latitudes.
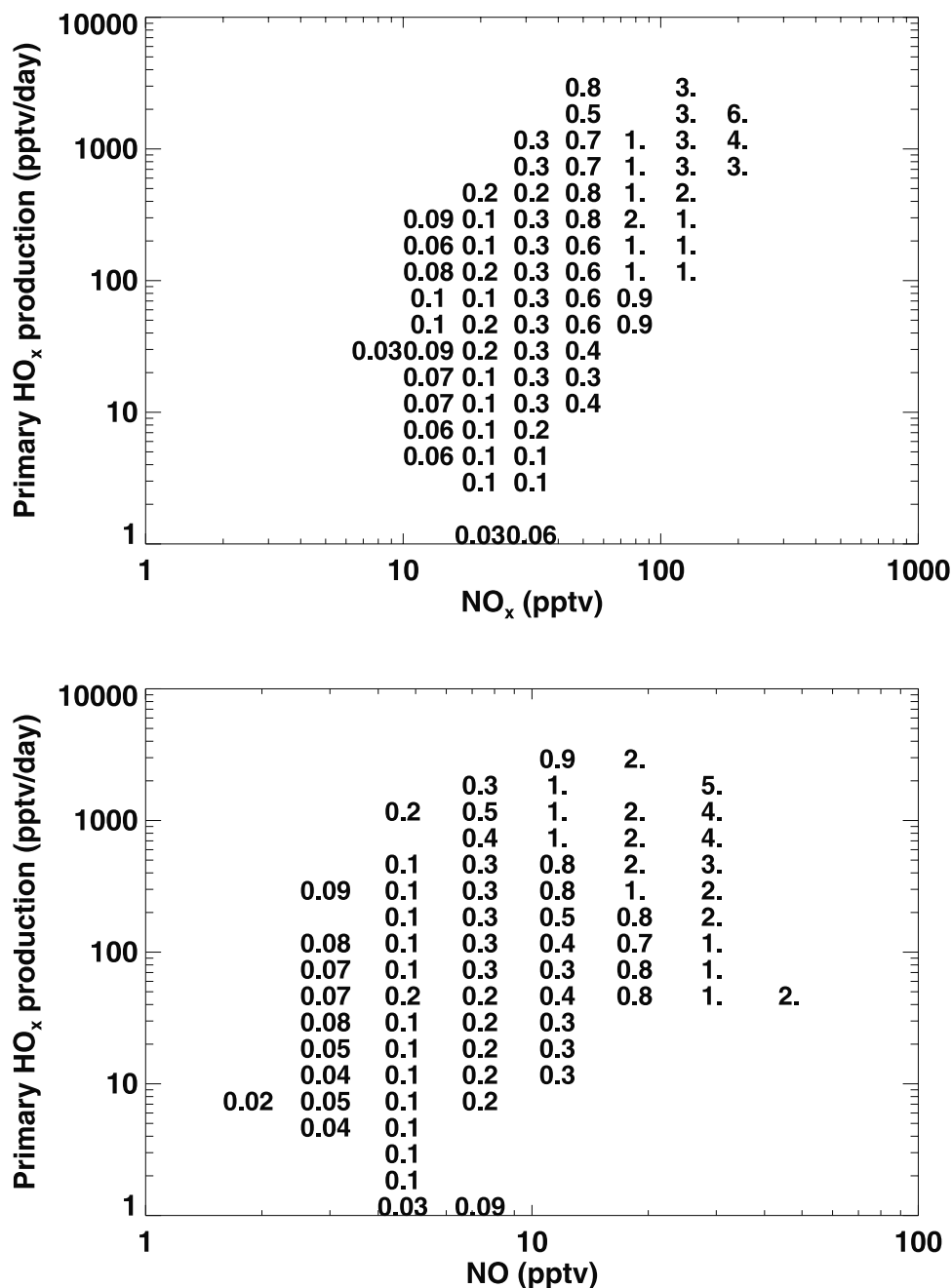
Figure 14. Numerical values of simulated 24-hour average O_3 production rates (ppbv/day) as a function of 24-hour average primary HO_x production and NO_x or NO concentrations. The primary HO_x production is from the reaction of $O(^1D)$ and H_2O and photolysis of acetone. Constraining the model with observed peroxide and CH_2O concentrations would yield similar results but with much fewer data.

higher OH concentrations at midlatitudes. The net loss of NO_x to PAN is also more significant at about 2 pptv/day at midlatitudes than a rate of about 1 pptv/day at high latitudes. The loss is larger at higher altitudes because of the strong temperature dependence of PAN thermal decomposition. Unlike in the tropics where PAN decomposition provides the main NO_x source in the lower troposphere [*Schultz et al.*, 1999; *Wang et al.*, 2001], PAN formation constitutes a net loss of NO_x at all altitudes during TOPSE. Reducing acetone concentrations in the model by 50% decreases the net loss of NO_x to PAN by 0.1–1 pptv/day at midlatitudes and <0.5 pptv/day at high latitudes. It

appears clear that the decomposition of long-lived nitrogen reservoirs cannot explain the observed seasonal increase of NO_x during TOPSE. *Carpenter et al.* [2000] also found that PAN decomposition did not contribute to NO_x concentrations at the Jungfraujoch Observatory (3.6 km above sea level) in the Swiss Alps during FREETEX'98. These results are consistent with the finding by *Wang et al.* [1998] in a global 3-D model study that PAN formation and decomposition generally does not contribute significantly to the observed springtime O_3 maxima over northern mid and high latitude continents. More measurements are necessary to understand if and how the NO_x source from PAN decom-
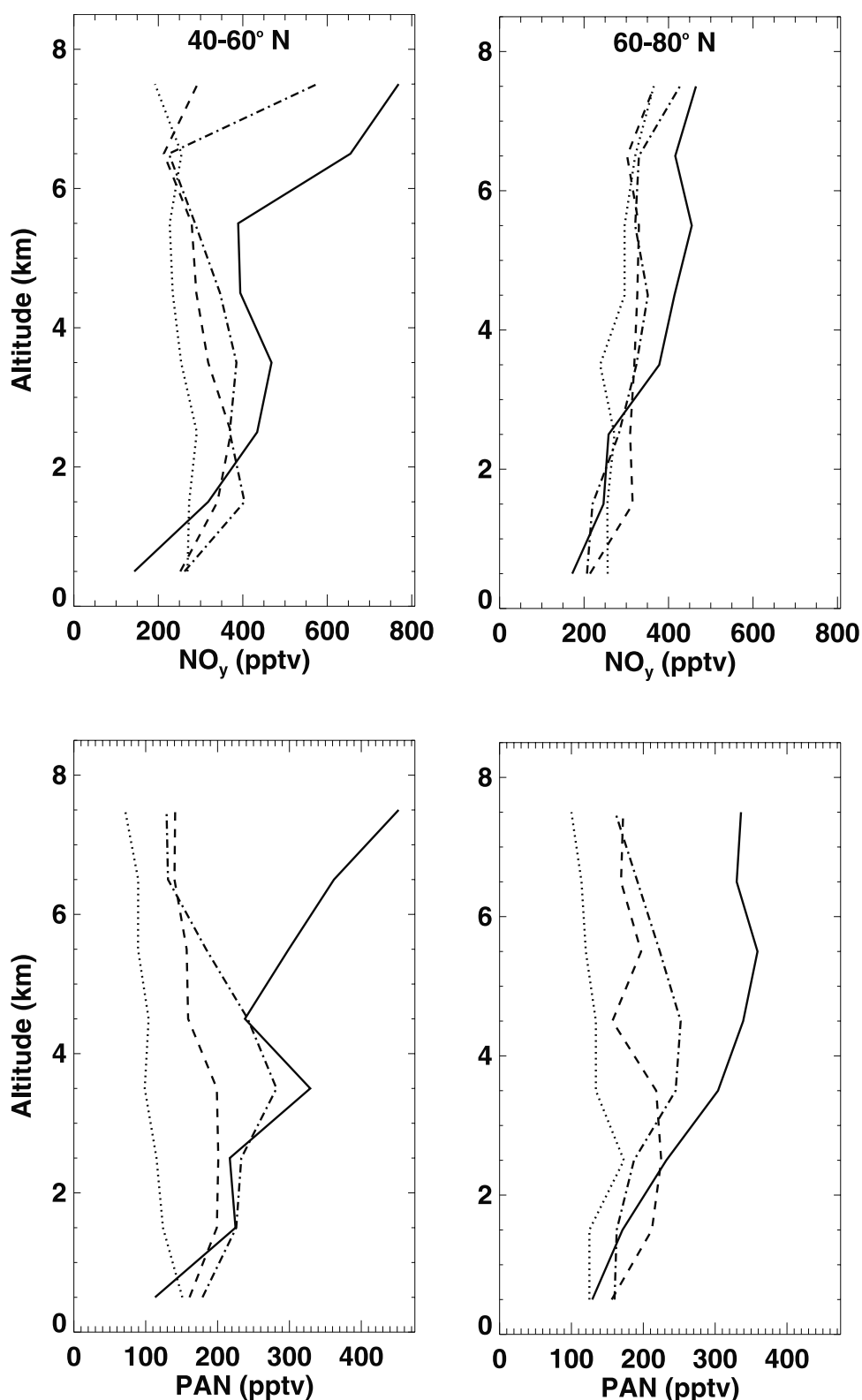
Figure 15. Same as Figure 1 but for NO_y, PAN, and DNO_y ($\equiv NO_y - (NO + NO_2 + PAN + PPN + HNO_3 + 2N_2O_5 + HNO_4)$). Medians of DNO_y for March and April are calculated mostly from a minimum of 10 data points. The data counts of DNO_y per altitude bin are less in February and May.

position in remote marine regions and lower latitudes contributes to the seasonal variability of ozone.

[36] The seasonal increases of NO and primary HO_x production (Figures 1 and 4) result in increasing chemical

production of O_3 (Figure 14). Figure 17 shows the budgets of O_3 at mid and high latitudes. The model is not constrained by observed peroxides or CH_2O because the restriction would reduce available data points so severely
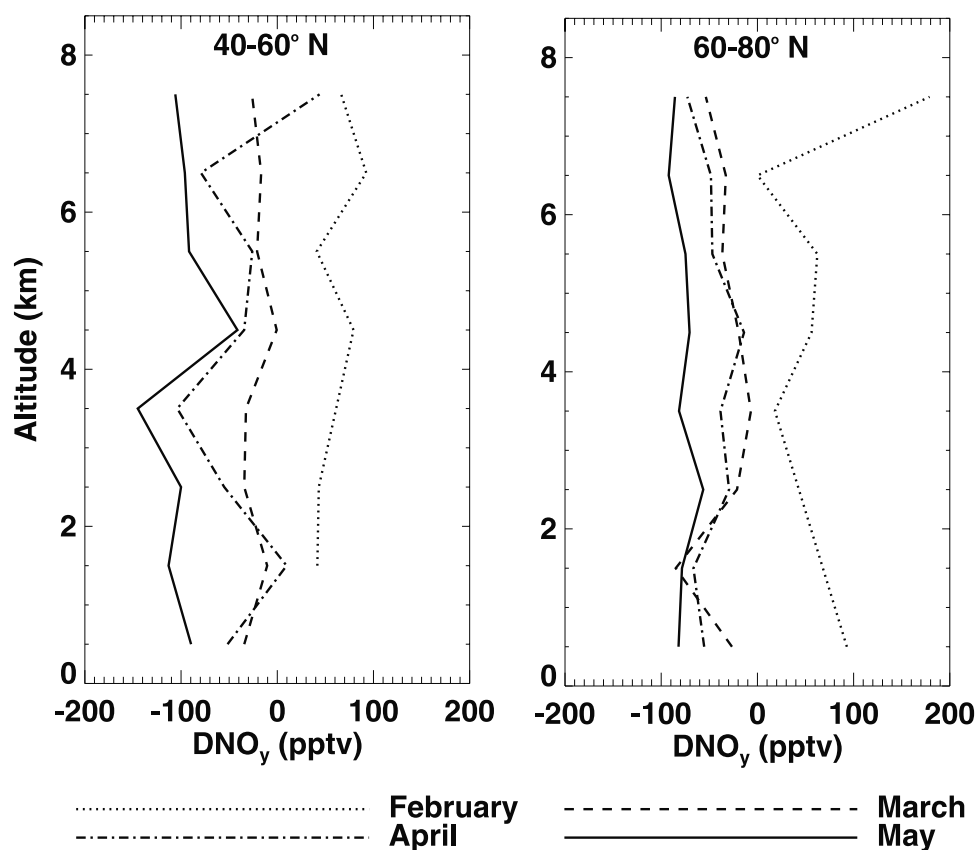
Figure 15. (continued)

that no statistically meaningful column budget can be obtained. The comparison of the simulations with and without the constraints shows that the effect of the scavenging loss of H_2O_2 is larger than those of higher than simulated ("excess") CH_3OOH and CH_2O concentrations in the observations. The resulting effects are similar (10–20% overestimates) for O_3 production, loss, and net production (loss).

[37] Figure 17 shows the rapid increase of O_3 production throughout the spring. The increase is more rapid at high latitudes (by a factor of 2–3 per month) than at midlatitudes (decreasing from a factor of 2 in February–March to 50% in April–May). By May, O_3 column production rates (0–8 km) are 3.2×10^{11} and 2.3×10^{11} cm^{-2} s^{-1} for mid and high latitudes, respectively. About 70% of O_3 production is due to the reaction of HO_2 and NO, and the rest is by the reactions of NO with CH_3O_2 and other organic peroxy radicals. The source from the reactions of NO and other organic peroxy radicals are significant compared to that from the reaction of NO and CH_3O_2 in early spring. The relative strengths of the two sources changes from 1:1 (1:2) in February to 1:3 (1:4) in May at high (mid) latitudes, reflecting the decrease of NMHCs with season (Figure 1). Our rate estimates are less than those calculated by *Cantrell et al.* [2002]; the former values are 24-hour averages while the latter ones are instantaneous rates at the time of the observations.

[38] The ozone budget at midlatitudes can be compared with the estimates for the western north Pacific ($30°–50°N$) in February–March (1994) by *Crawford et al.* [1997]. They found much larger column O_3 production (10.5×10^{10}

cm^{-2} s^{-1}) than loss (3.8×10^{10} cm^{-2} s^{-1}). Their production rate is similar to our estimate for March but their loss rate is similar to our estimate in February. As a result, their estimated column net production is much larger than our estimate. The discrepancy is due in part to higher O_3 concentrations (~ 20 ppbv) during TOPSE. One important similarity between the two studies is that the lower free troposphere (1–4 km) is a significant region of net O_3 production. *Crawford et al.* [1997] attributed the enhanced O_3 production at these altitudes to continental outflow to the western Pacific.

[39] The dominant role that HO_2 plays in O_3 loss rates is shown in Figure 18. The largest loss of O_3 in the tropical and subtropical regions is due to photolysis of O_3 and the subsequent reaction of $O(^1D)$ and H_2O [e.g., *Davis et al.*, 1996; *Jacob et al.*, 1996]. In comparison, during TOPSE the largest loss of O_3 is from the reaction of O_3 and HO_2. At midlatitudes, that loss accounts for 70% of the total O_3 loss in February and a smaller 45% in May. *Kotchenruther et al.* [2001] reported a fraction of about 60% in April over the north eastern Pacific. The fractional contribution by the reaction of O_3 and HO_2 at high latitudes decreases from 90% in February to 70% in May. The highest contribution by the reaction of $O(^1D)$ and H_2O is 35% at midlatitudes in May. The small fractional contribution to O_3 loss by the reaction of $O(^1D)$ and H_2O reflects much drier air and less solar insolation over the TOPSE region compared to the lower latitudes. The crucial role played by HO_2 in both O_3 production and loss explains the similar sensitivities of these variables to a change in the HO_x source.
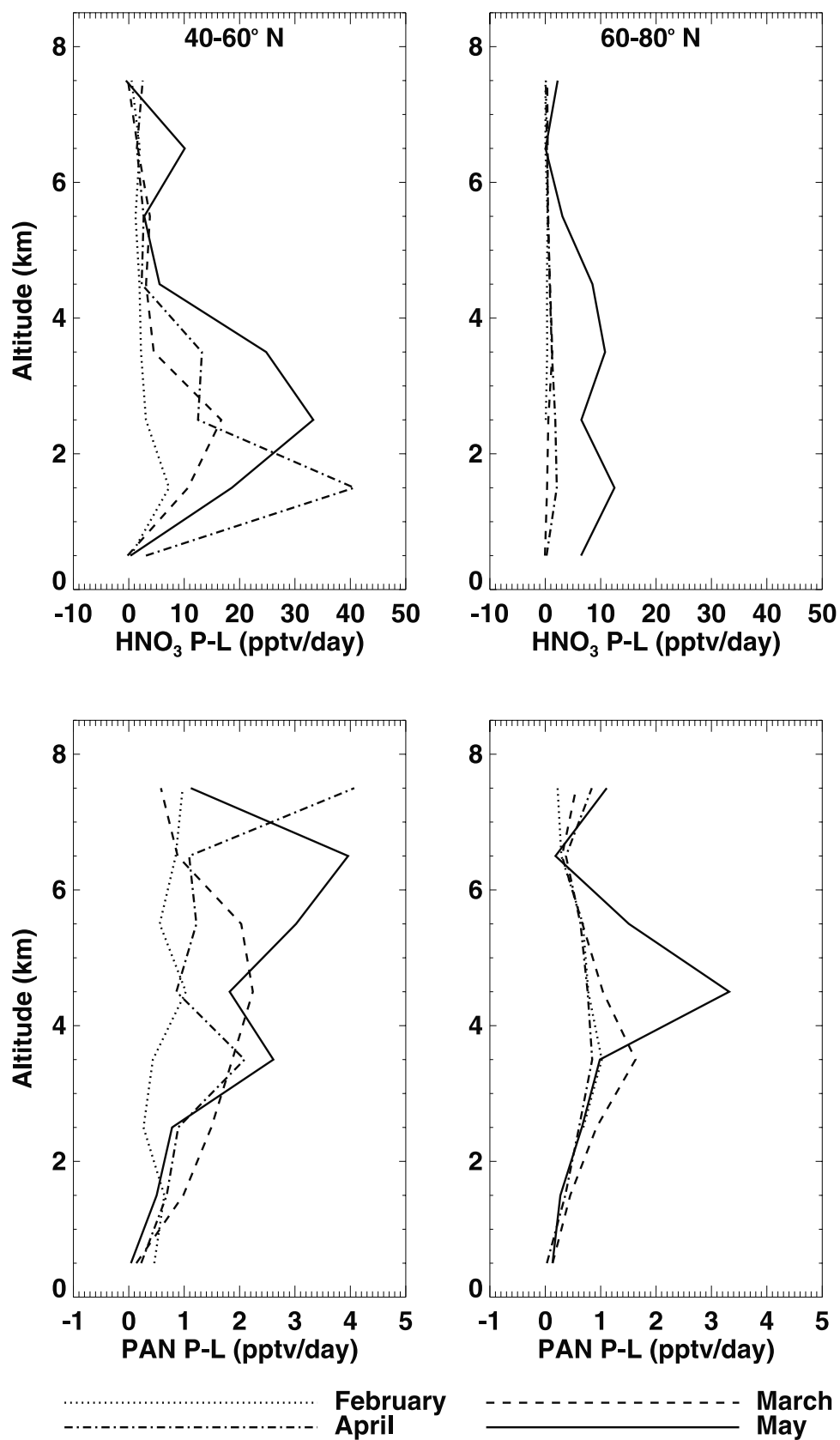
Figure 16. Same as Figure 1 but for simulated 24-hour average net production rates of HNO_3 and PAN. The model is constrained by observed HNO_3 and PAN concentrations.
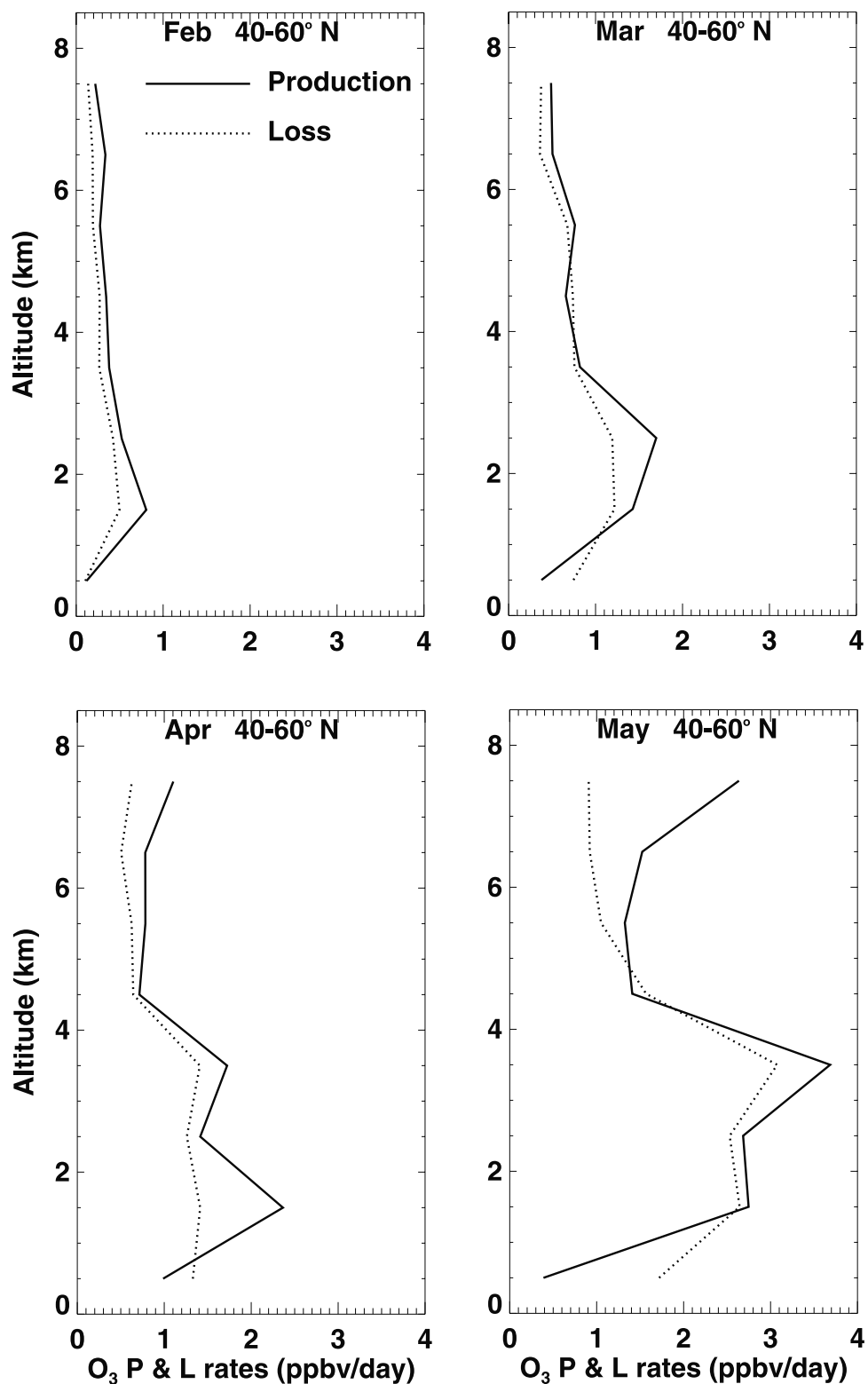
Figure 17. Simulated monthly medians of 24-hour average O_3 production and loss rates as a function of altitude at mid and high latitudes. A median value plotted represents a minimum of 10 data points. The column (0−8 km) O_3 production rates at mid (high) latitudes are 6.3 (0.8), 14 (2.7), 21 (8.0), and 32 (23) $\times$ 10^{10} cm^{-2} s^{-1} for February, March, April, and May, respectively. The corresponding loss rates are 4.4 (0.9), 13 (2.7), 17 (9.0), and 31 (20) $\times$ 10^{10} cm^{-2} s^{-1}.
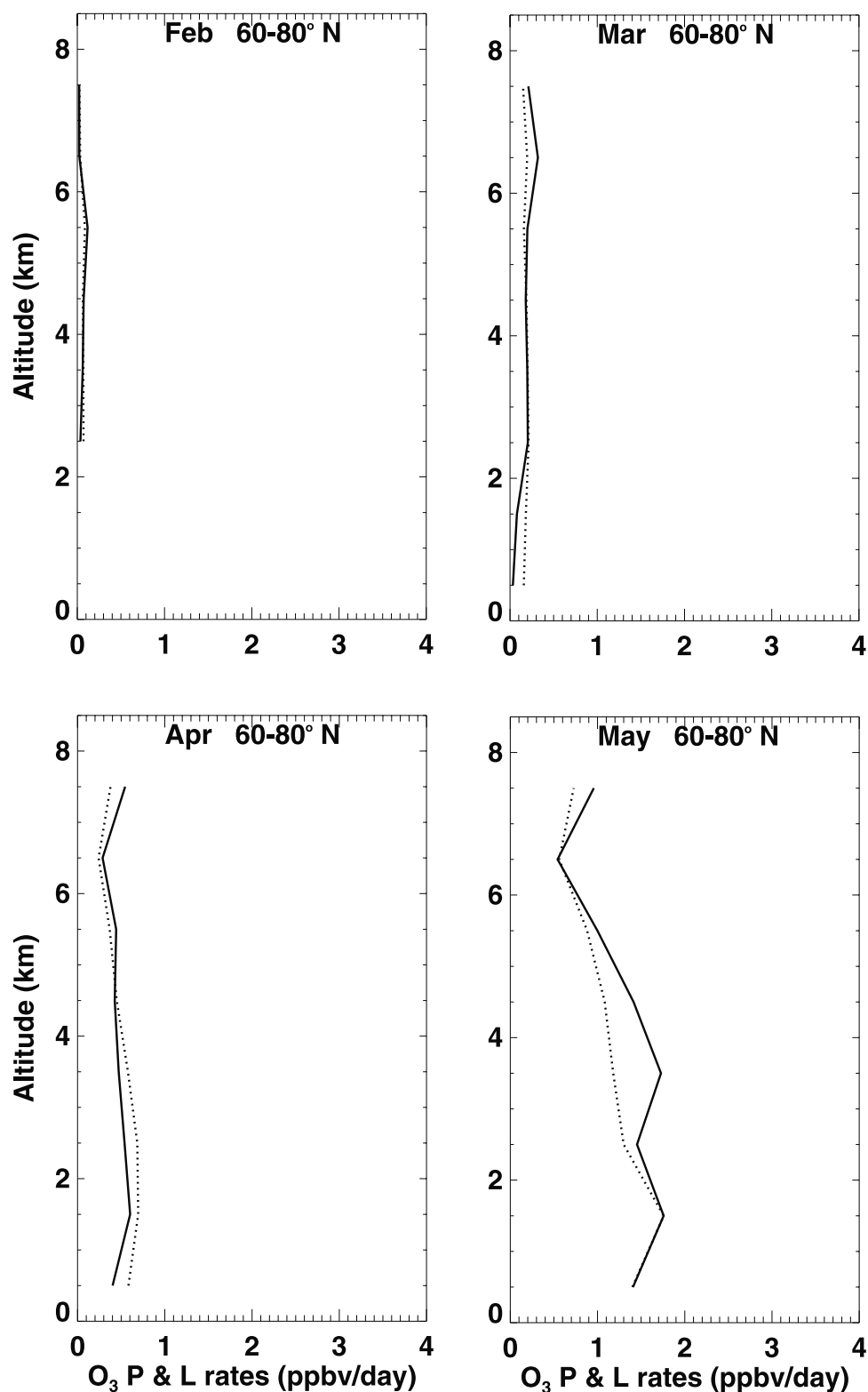
Figure 17. (continued)

[40] The relatively small loss of O_3 by the reaction of $O(^1D)$ and H_2O helps limit O_3 loss at northern mid and high latitudes in spring, resulting in a net chemical production of O_3 at midlatitudes during TOPSE. At midlatitudes, the net column chemical production is 2×10^{10}, 1×10^{10}, 4×10^{11}, and 1×10^{11} cm^{-2} s^{-1} for February, March, April,

and May respectively. The corresponding values at high latitudes are -6×10^8, -4×10^9, -1×10^{10}, and 3×10^{10} cm^{-2} s^{-1}. The net loss in February–April at high latitudes reflects the low NO_x concentrations (<5 pptv below 5 km) in the region (Figure 1). The net chemical production or loss is only 3–20% of the column O_3 production or loss rate at
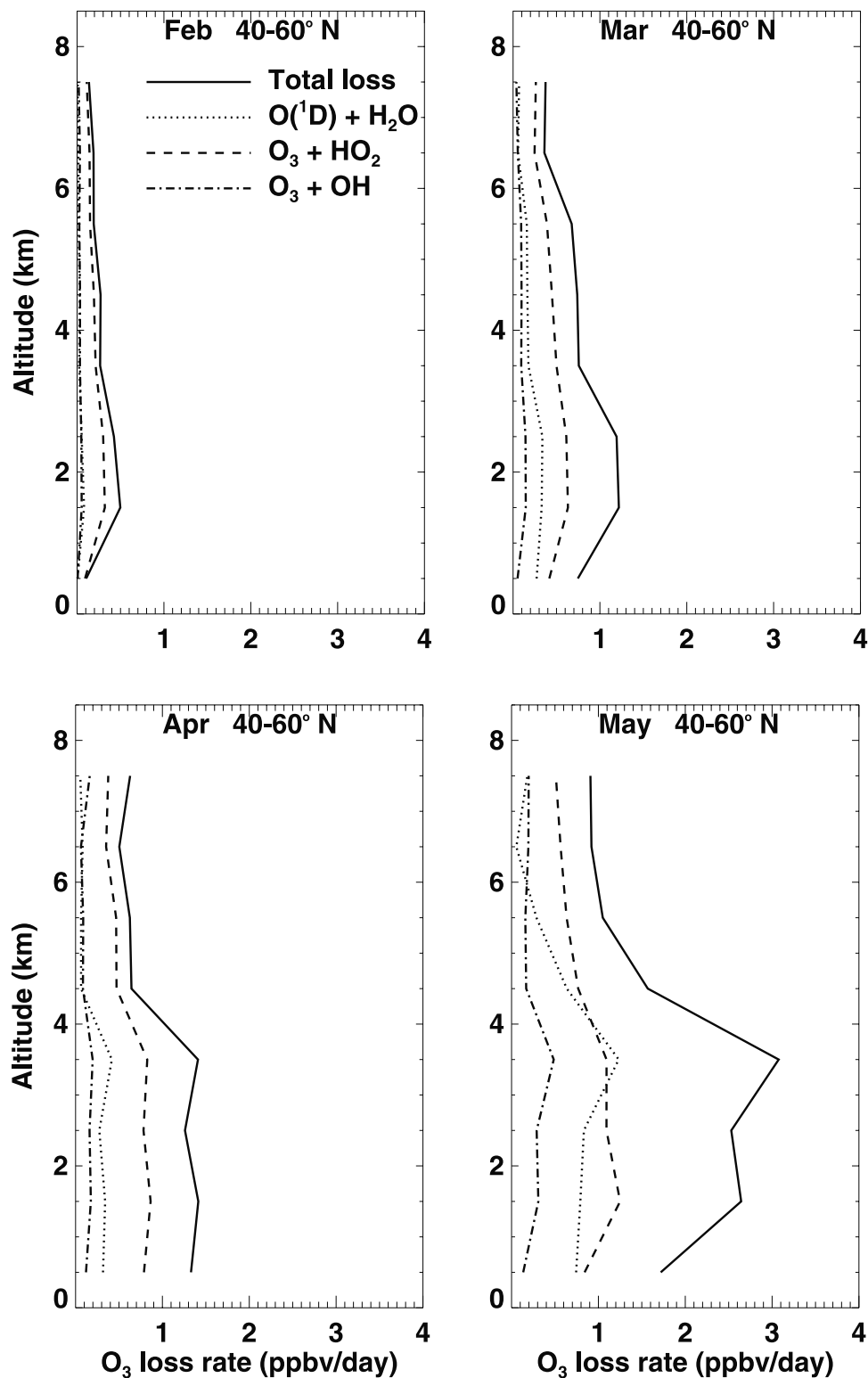
Figure 18. Same as Figure 17 but for simulated 24-hour average loss rates of O_3 from various pathways.

0–8 km. The combination of high NO concentrations and low H_2O content leads to net O_3 production at high altitudes. Including the net O_3 production in the region between 8 km and the tropopause will further increase the estimated net chemical production of O_3.

[41] Figure 19 shows that the median column O_3 concentration (defined as column moles of O_3/column moles of air) at midlatitudes is highest in April and that the most rapid O_3 increase occurs in March–April, a period when the springtime O_3 maxima were observed at lower altitudes at
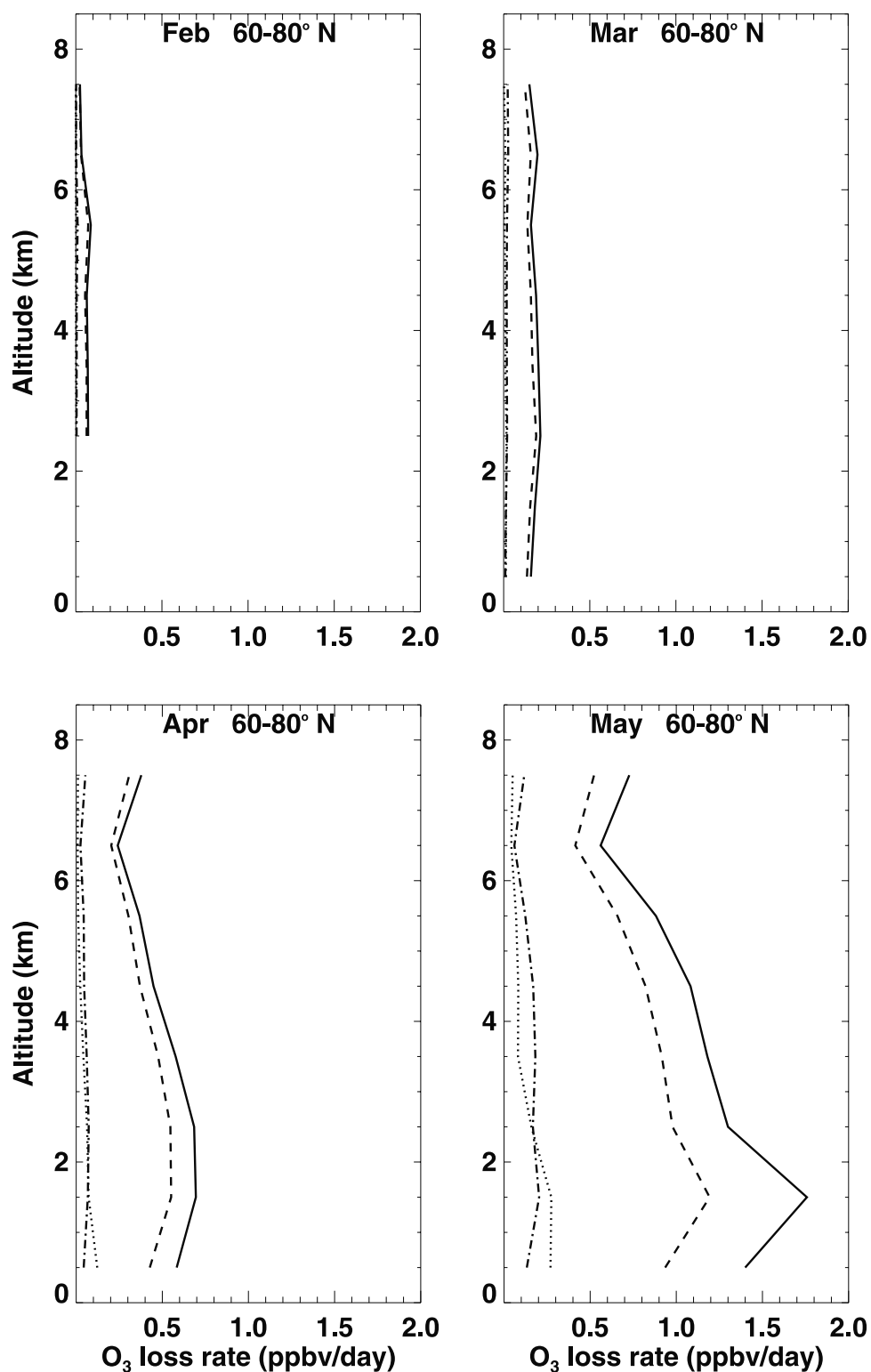
Figure 18.   (continued)

mid and high latitudes [e.g., *Logan*, 1985; *Levy et al.*, 1985]. The estimated net O_3 production is also largest in April. In contrast, at high latitudes during TOPSE, column O_3 concentrations continue to increase from February to May and there is an estimated chemical loss of O_3 from February to April. To illustrate the different effects of in situ

net O_3 chemical production (loss) on column O_3 concentrations at mid and high latitudes, we show in Figure 19 the column concentrations of O_3 for March, April, and May if in situ chemistry is the only factor influencing the concentrations (see also the figure caption). The estimated column O_3 at midlatitudes does not show a maximum in April

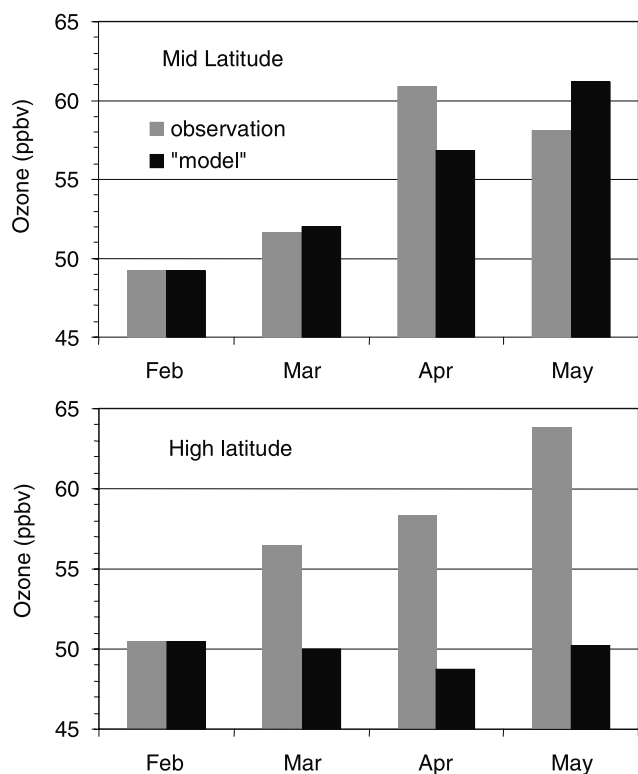**Figure 19.** Observed median O$_3$ column mixing ratios as a function of month at mid and high latitudes. For "modeled" column mixing ratios, we start from the observed February values on February 14 and compute the subsequent mixing ratios in the middle of March, April, and May using simulated monthly medians of 24-hour average net production (loss) rates.

because the in situ chemical production is still larger than loss in May. Nonetheless, the estimated concentrations reach the observed levels at midlatitudes. In comparison, the estimated O$_3$ concentrations at high latitudes remain at about 50 ppbv due to the relatively small net production or loss in that region, whereas the observed column mixing ratio increases by 15 ppbv.

[42] In situ chemistry alone cannot explain the observed springtime O$_3$ maxima at northern mid and high latitudes; transport plays an important role. *Wang et al.* [1998] tagged O$_3$ transported from the stratosphere and that produced in different regions of the troposphere in a global 3-D chemistry and transport model. They found that O$_3$ from the stratosphere peaked in late winter and early spring whereas O$_3$ produced from the troposphere peaked in late spring and early summer. Both sources are important in reproducing the observed springtime O$_3$ maxima at remote northern mid and high latitude sites in their model. *Yienger et al.* [1999] emphasized the role played by the net O$_3$ chemical production at midlatitudes, which we find to be important for the TOPSE region. Their simulated net chemical O$_3$ production (2–10 km) at midlatitudes peaks in March, one month earlier than we find for the TOPSE region. The two results, however, cannot be directly compared because their results include all regions at 30°–60°N. In our current work, we focused only on the

effects of in situ chemical production and loss during TOPSE. Detailed analysis of tropospheric and stratospheric O$_3$ transport into the TOPSE region is presented by *Allen et al.* [2002], *Browell et al.* [2002], *Dibb et al.* [2002], L. K. Emmons et al. (The budget of tropospheric ozone during TOPSE from two CTMs, submitted to *Journal of Geophysical Research*, 2002), and Y. Wang et al. (Intercontinental transport of pollution manifested in the seasonal trend of springtime O$_3$ at northern mid and high latitudes, submitted to *Science*, 2002).

6. Conclusions

[43] Measurements were made onboard the NCAR/NSF C-130 aircraft in February–May during the TOPSE experiment at northern mid and high latitudes. The temporal and spatial span of the measurements allows for analysis of the rapid transition of photochemistry in springtime using a photochemical model. We have focused our work on photochemical factors driving HO$_x$ and O$_3$ chemistry.

[44] The continuously decreasing concentrations of NMHCs through spring, due in part to increasing OH oxidation, contrast to the observed increase in O$_3$ and NO concentrations. Both trends favor partitioning of HO$_x$ toward OH. Photochemical activity as measured by the sources of HO$_x$ increases rapidly at mid and high latitudes with season. The primary driving force for radical chemistry is photolysis of O$_3$ and the subsequent reaction of O(^{1}D) and H$_2$O, which benefits not only from the increasing solar insolation but higher H$_2$O content of the warming air. The concentrations of total peroxy radicals rise accordingly; observed and simulated concentrations are in good agreement.

[45] One feature that sets TOPSE apart from the other tropospheric field experiments is the observations of low H$_2$O$_2$ concentrations (by a factor of 2–10) compared to model estimates. The loss of HO$_x$ required to match observed H$_2$O$_2$ concentrations in the model implies a loss of 20–30% and 10–20% in OH concentrations and O$_3$ production, respectively. The timescale of scavenging by rainout, calculated from the observed HNO$_3$ concentrations, increases from about 1 week at midlatitudes to 2–4 weeks at high latitudes in agreement with previous estimates. However, the required scavenging loss frequency of H$_2$O$_2$ is much faster. Furthermore, it increases rapidly with season. The estimated timescales of H$_2$O$_2$ against scavenging loss in May are about half a day and 1 day at mid and high latitudes, respectively. If the scavenging loss of H$_2$O$_2$ were mostly due to its oxidation of SO$_2$ in droplets, the oxidation would imply a sulfate deposition rate of >2.5 g S m^{-2} yr^{-1}, an order of magnitude larger than previous estimates. Unknown mechanisms need to be invoked to explain the rapid loss of H$_2$O$_2$ during TOPSE.

[46] Whereas observed and simulated CH$_3$OOH concentrations show good agreement in April and May at high latitudes, they differ significantly in March at midlatitudes. The model shows generally decreasing CH$_3$OOH concentrations with altitudes; an opposite trend is observed in March at midlatitudes. Transport processes alone do not appear to explain the observed profile of increasing CH$_3$OOH concentrations with altitude. Using observed in place of simulated CH$_3$OOH concentrations in the model tends to increase CH$_2$O concentrations at high altitudes. The

relative enhancement is significant (50–100% or 20–30 pptv) at 6–8 km in March.

[47] Observed and simulated CH_2O concentrations show better agreement than in previous northern midlatitude missions. The consistent underestimates by the model in the upper troposphere at high altitudes imply a large source of HO_x (by CH_2O photolysis) in the region. Likely sources are transport from midlatitudes or heterogeneous conversion from methanol or other species, in which case photolysis of CH_2O boosts the primary production of HO_x. This additional HO_x source increases the total HO_x production by 50–200% at 6–8 km at high latitudes resulting in 10–50% increases in OH concentrations and O_3 production.

[48] The source of NO_x does not appear to come from the decomposition of long-lived reactive nitrogen species, among which PAN is the most dominant component. The tropospheric burden of NO_y at mid and high latitudes continues to grow throughout the spring. This seasonal increase is clearly evident in the free troposphere. The seasonality is less clearly defined at 0–3 km. The concentrations of NO_y near the surface decrease from February to May (particularly at high latitudes) as those of NMHCs. Similar difference of the seasonal trend with altitude is observed for PAN except that the seasonal peak of PAN near the surface shifts toward April. Budget studies of PAN and HNO_3 show a net loss of NO_x to these reservoirs species throughout the spring. There appears to be a seasonal shift in the difference between NO_y and the sum of individual components ($NO + NO_2 + PAN + PPN + HNO_3 + 2N_2O_5 + HNO_4$), among which NO_2, N_2O_5, and HNO_4 are computed in the model. The former is larger in February but becomes progressively smaller than the latter in later months. The shift shows little altitude dependence.

[49] The production of O_3 in the TOPSE region increases substantially from February to May, by factors of 5 and 25 respectively at mid and high latitudes. The rapid increase is driven by increasing primary HO_x production and NO concentrations. The latter is due in part to the increasing partitioning of NO_x toward NO with more intense solar irradiation in spring. Ozone production is less sensitive to an increase in the primary HO_x production than that in NO concentrations. However, the former factor, driven by the reaction of $O(^1D)$ and H_2O, increases more rapidly than the latter. Ozone photochemistry is in the NO_x-limited regime during TOPSE.

[50] Peroxy radicals generally play the pivotal role in O_3 production. The reaction of HO_2 and NO accounts for about 70% of the total production. The contribution by the reaction of higher ($\geq C_2$) organic peroxy radicals and NO is as large as that by the reaction of CH_3O_2 and NO in early spring, reflecting the high concentrations of NMHCs at the time. Its relative importance decreases toward summer. During TOPSE, HO_2 is also the major component in O_3 loss through the reaction of HO_2 and O_3. The loss pathway accounts for 45–70% and 70–90% of the total loss at mid and high latitudes, respectively. The loss pathway by photolysis of O_3 and the subsequent reaction of $O(^1D)$ and H_2O, which dominates O_3 loss at lower latitudes, is highest (35%) at midlatitudes in May. As a result, the sensitivities of O_3 production and loss to a change in the primary HO_x production are similar.

[51] We find net in situ column O_3 chemical production (0–8 km) at midlatitudes, 2×10^{10}, 1×10^{10}, 4×10^{11}, and 1×10^{11} cm^{-2} s^{-1} for February, March, April, and May respectively. In contrast, there is a net in situ chemical loss of O_3 at high latitudes except in May. The corresponding values at high latitudes are -6×10^8, -4×10^9, -1×10^{10}, and 3×10^{10} cm^{-2} s^{-1}. The difference reflects lower NO concentrations and solar irradiation at high latitudes. At midlatitudes, the lower free troposphere (1–4 km) in addition to the upper troposphere is a region of significant net O_3 production. The observed O_3 column (0–8 km) shows a peak in April at midlatitudes but continues to increase from February to May at high latitudes. In situ chemistry alone cannot explain the observed seasonality of column O_3 during TOPSE. Nonetheless, in situ net chemical production is a significant contributor to the observed O_3 increase at midlatitudes, where both net O_3 production and column concentration peak in April. Net transport from other tropospheric regions or the stratosphere is necessary to explain the observed seasonal increase of column O_3 at high latitudes.

References

Allen, J. J., J. E. Dibb, K. E. Pickering, and B. A. Ridley, An estimate of the stratospheric contribution to springtime tropospheric ozone maxima using TOPSE measurements and Beryllium-7 simulations, *J. Geophys. Res.*, doi:10.1029/2001JD001428, in press, 2002. [printed *108*(D8), 2003]

Atkinson, R., et al., Evaluated kinetic and photochemical data for atmospheric chemistry, *J. Phys. Chem. Ref. Data*, 26, 1329–1499, 1997.

Ayers, G. P., R. W. Gillett, H. Granek, C. de Serves, and R. A. Cox, Formaldehyde production in clean marine air, *Geophys. Res. Lett.*, 24, 401–404, 1997.

Balkanski, Y. J., D. J. Jacob, G. M. Gardner, W. M. Graustein, and K. K. Turekian, Transport and residence times of continental aerosols inferred from a global 3-dimensional simulation of ^{210}Pb, *J. Geophys. Res.*, 98, 20,573–20,586, 1993.

Blake, N. J., D. R. Blake, B. C. Sive, A. S. Katzenstein, S. Meinardi, O. W. Wingenter, E. L. Atlas, F. Flocke, B. A. Ridley, and F. S. Rowland, The seasonal evolution of NMHCs and light alkyl nitrates at mid to high northern latitudes during TOPSE, *J. Geophys. Res.*, doi:10.1029/2001JD001467, in press, 2002. [printed *108*(D8), 2003]

Bottenheim, J. W., and M. F. Shepherd, C2-C6 hydrocarbon measurements at 4 rural locations across Canada, *Atmos. Environ.*, 29, 647–664, 1995.

Bradshaw, J., et al., Observed distributions of nitrogen oxides in the remote free troposphere from the NASA Global Tropospheric Experiment programs, *Rev. Geophys.*, 38, 61–116, 2000.

Browell, E., et al., Ozone, aerosol, potential vorticity, and trace gas trends observed at high latitudes over Northern America from February to May 2000, *J. Geophys. Res.*, doi:10.1029/2001JD001390, in press, 2002. [printed *108*(D4), 2003]

Cantrell, C., et al., Steady state free radical budgets and ozone photochemistry during TOPSE, *J. Geophys. Res.*, doi:10.1029/2002JD002198, in press, 2002. [printed *108*(D8), 2003]

Carpenter, L. J., et al., Oxidized nitrogen and ozone production efficiencies in the springtime free troposphere over the Alps, *J. Gephys. Res.*, 105, 14,547–14,559, 2000.

Chen, G., et al., An assessment of HO_x chemistry in the tropical Pacific boundary layer: Comparison of observations with model simulations during PEM Tropics A, *J. Atmos. Chem.*, 38, 317–344, 2001.

Christensen, L. E., M. Okumura, S. P. Sander, R. J. Salawitch, G. C. Toon, B. Sen, J.-F. Blavier, and K. W. Jucks, Kinetics of $HO_2 + HO_2 \rightarrow H_2O_2 + O_2$: Implications for Stratospheric H_2O_2, *Geophys. Res. Lett.*, 29(9), 1299, doi:10.1029/2001GL014525, 2002.

Crawford, J. H., et al., An assessment of ozone photochemistry in the extratropical western North Pacific: Impact of continental outflow during the late winter/early spring, *J. Geophys. Res.*, *102*, 28,469–28,487, 1997.

Crawford, J. H., et al., Assessment of upper tropospheric HO_x sources, *J. Geophys. Res.*, *104*, 16,255–16,273, 1999.

Davis, D. D., et al., Assessment of the ozone photochemistry tendency in the western North Pacific as inferred from PEM-West A observations during the fall of 1991, *J. Geophys. Res.*, *101*, 2111–2134, 1996.

Davis, D. D., et al., Marine latitude/altitude OH distributions: Comparison of Pacific Ocean observations with models, *J. Geophys. Res.*, *106*, 32,691–32,708, 2001.

DeMore, W. B., et al., *Chemical Kinetics and Photochemical Data for Use in Stratospheric Modeling*, JPL Publ. 97-4, 266 pp., Jet Propulsion Lab., Pasadena, Calif., 1997.

Dibb, J. E., R. W. Talbot, E. M. Scheuer, G. Seid, L. DeBell. B. Lefer, and B. A. Ridley, Stratospheric influence on the northern North American free troposphere during TOPSE: [7]Be as a stratospheric tracer, *J. Geophys. Res.*, doi:10.1029/2001JD001347, in press, 2002. [printed *108*(D4), 2003]

Fried, A., et al., Tunable diode laser measurements of formaldehyde during the TOPSE 2000 study: Distributions, trends, and model comparisons, *J. Geophys. Res.*, doi:10.1029/2002JD002208, in press, 2002. [printed *108*(D8), 2003]

Hoffmann, M. R., and J. O. Edwards, Kinetics of oxidation of sulfite by hydrogen peroxide in acidic solution, *J. Phys. Chem.*, *79*, 2096–2098, 1975.

Honrath, R. E., and D. A. Jaffe, The seasonal cycle of nitrogen oxides in the Arctic troposphere at Barrow, Alaska, *J. Geophys. Res.*, *97*, 20,615–20,630, 1992.

Honrath, R. E., A. J. Hamlin, and J. T. Merrill, Transport of ozone precursors from the Arctic troposphere to the North Atlantic region, *J. Geophys. Res.*, *101*, 29,335–29,351, 1996.

Jacob, D. J., et al., The origin of ozone and NO_x in the tropical troposphere: A photochemical analysis of aircraft observations over the South Atlantic Basin, *J. Geophys. Res.*, *101*, 24,235–24,250, 1996.

Jacob, D. J., B. D. Field, E. Jin, I. Bey, Q. Li, J. A. Logan, and R. M. Yantosca, Atmospheric budget of acetone, *J. Geophys. Res.*, *107*(D9), 4100, doi:10.1029/2001JD000694, 2002.

Jaeglé, L., et al., Ozone production in the upper troposphere and the influence of aircraft during SONEX: Approach of NO_x-saturated conditions, *Geophys. Res. Lett.*, *26*, 3081–3084, 1999.

Jaeglé, L., et al., Photochemistry of HO_x in the upper troposphere at northern midlatitudes, *J. Geophys. Res.*, *105*, 3877–3892, 2000.

Jobson, B. T., et al., Measurements of C2-C6 hydrocarbons during the Polar Sunrise 1992 Experiment: Evidence for Cl atom and Br atom chemistry, *J. Geophys. Res.*, *99*, 25,355–25,368, 1994.

Kotchenruther, R. A., D. A. Jaffe, and L. Jaeglé, Ozone photochemistry and the role of peroxyacetyl nitrate in the springtime northeastern Pacific troposphere: Results from the Photochemical Ozone Budget of the Eastern Northern Pacific Atmosphere (PHOBEA) Campaign, *J. Geophys. Res.*, *106*, 28,731–28,742, 2001.

Langer, J., and H. Rodhe, A global three-dimensional model of the tropospheric sulfur cycle, *J. Atmos. Chem.*, *13*, 225–263, 1991.

Levy, H., II, J. D. Mahlman, W. J. Moxim, and S. C. Liu, Tropospheric ozone: The role of transport, *J. Geophys. Res.*, *88*, 3753–3772, 1985.

Liu, S. C., M. Trainer, F. C. Fehsenfeld, D. D. Parrish, E. J. Williams, D. W. Fahey, G. Hubler, and P. C. Murphy, Ozone production in the rural troposphere and the implications for regional and global ozone distributions, *J. Geophys. Res.*, *92*, 10,463–10,482, 1987.

Liu, S. C., et al., A study of the photochemistry and ozone budget during the Mauna Loa Observatory Photochemistry Experiment, *J. Geophys. Res.*, *97*, 10,463–10,471, 1992.

Logan, J. A., Tropospheric ozone: Seasonal behavior, trends, and anthropogenic influence, *J. Geophys. Res.*, *90*, 10,463–10,482, 1985.

Logan, J. A., M. J. Prather, S. C. Wofsy, and M. B. McElroy, Tropospheric chemistry: A global perspective, *J. Geophys. Res.*, *86*, 7210–7254, 1981.

McKeen, S. A., et al., Photochemical modeling of hydroxyl and its relationship to other species during the tropospheric OH photochemistry experiment, *J. Geophys. Res.*, *102*, 6467–6493, 1997.

Novelli, P. C., J. E. Collins Jr., R. C. Myers, G. W. Sachse, and H. E. Scheel, Re-evaluation of the NOAA/CMDL carbon monoxide reference scale and comparisons to CO reference gases at NASA-Langley and the Fraunhofer Institute, *J. Geophys. Res.*, *99*, 12,833–12,839, 1994.

Penkett, S. A., and K. A. Brice, The spring maximum in photo-oxidants in the Northern Hemisphere troposphere, *Nature*, *319*, 655–657, 1986.

Prather, M. J., and D. J. Jacob, A persistent imbalance in HO_x and NO_x photochemistry of the upper troposphere driven by deep tropical convection, *Geophys. Res. Lett.*, *24*, 3189–3192, 1997.

Schultz, M., et al., On the origin of tropospheric ozone and NO_x over the tropical South Pacific, *J. Geophys. Res.*, *104*, 5829–5843, 1999.

Shetter, R. E., L. Cinquini, B. L. Lefer, S. R. Hall, and S. Madronich, Comparison of airborne measured and calculated spectral actinic flux and derived photolysis frequencies during the PEM Tropics B mission, *J. Geophys. Res.*, *107*, 8234, doi:10.1029/2001JD001320, 2002. [printed *108*(D2), 2003]

Singh, H., et al., Distribution and fate of selected oxygenated organic species in the troposphere and lower stratosphere over the Atlantic, *J. Geophys. Res.*, *105*, 3795–3805, 2000.

Talukdar, R. K., C. A. Longfellow, M. K. Gilles, and A. R. Ravishankara, Quantum yields of $O(^1D)$ in the photolysis of ozone between 289 and 329 nm as a function of temperature, *Geophys. Res. Lett.*, *25*, 143–146, 1998.

Tie, X., et al., Effect of sulfate aerosol on tropospheric NO_x and ozone budgets: Model simulations and TOPSE evidence, *J. Geophys. Res.*, doi:10.1029/2001JD001508, in press, 2002. [printed *108*(D2), 2003]

Wang, Y., D. J. Jacob, and J. A. Logan, Global simulation of tropospheric O_3-NO_x-hydrocarbon chemistry, 3, Origin of tropospheric ozone and effects of non-methane hydrocarbons, *J. Geophys. Res.*, *103*, 10,757–10,768, 1998.

Wang, Y., S. C. Liu, H. Yu, S. Sandholm, T.-Y. Chen, and D. R. Blake, Influence of convection and biomass burning on tropospheric chemistry over the tropical Pacific, *J. Geophys. Res.*, *105*, 9321–9333, 2000.

Wang, Y., et al., Factors Controlling Tropospheric O_3, OH, NO_x, and SO_2 over the Tropical Pacific during PEM-Tropics B, *J. Geophys. Res.*, *106*, 32,733–32,748, 2001.

Yienger, J. J., A. A. Klonecki, H. Levy, W. J. Moxim, and G. R. Carmichael, An evaluation of chemistry's role in the winter-spring ozone maximum found in the northern midlatitude free troposphere, *J. Geophys. Res.*, *104*, 3655–3668, 1999.

Zanis, P., P. S. Monks, E. Schuepbach, and S. A. Penkett, The role of in situ photochemistry in the control of ozone during spring at the Jungfraujoch (3580 m asl): Comparison of model results with measurements, *J. Atmos. Chem.*, *37*, 1–27, 2000.

E. Atlas, C. Cantrell, M. Coffey, F. Flocke, A. Fried, B. Lefer, B. Ridley, R. Shetter, J. Walega, A. Weinheimer, and B. Wert, National Center for Atmospheric Research, Boulder, CO, USA.

D. Blake and N. Blake, Department of Chemistry, University of California at Irvine, Irvine, CA, USA.

G. Chen, D. Davis, and Y. Wang, School of Earth and Atmospheric Sciences, Georgia Institute of Technology, Atlanta, GA 30332-0340, USA. (ywang@eas.gatech.edu)

J. Dibb and R. Talbot, Institute for the Study of Earth, Oceans, and Space, University of New Hampshire, Durham, NH, USA.

B. Heikes and J. Snow, Graduate School of Oceanography, University of Rhode Island, Narragansett, RI, USA.